Energy transfer

Photoinduced energy transfer

An important overall mechanism which is responsible for the quenching of molecular emission involves the transfer of excitation energy to the quencher in a bimolecular process:

$$\mathrm{M}^* + \mathrm{Q} \longrightarrow \mathrm{M} + \mathrm{Q}^*$$

This process is also referred to as a photosensitization reaction, in the sense that *Q* is excited without actually having to absorb a photon. This kind of process has a lot of applications in photochemistry, but can also be used to obtain different emission colors using one and the same excitation source.

There are different mechanisms that can lead to the transfer of energy from M to Q. One condition is certainly that the excitation energy of *Q** must be lower than or equal to that of *M**. The different processes may be classified according to:

$$\mathrm{M}^* \longrightarrow \mathrm{M} + h\nu \qquad \mathrm{Q} + h\nu \longrightarrow Q^*$$

- Radiative energy transfer in which the emission from M* is reabsorbed by Q:
  This process requires that the emission spectrum of M* overlaps with the absorption spectrum of *Q*.
- Nonradiative energy transfer in which a specific interaction between *M** and *Q* is required. Two types of interaction may be identified which are termed Coulomb and electron-exchange energy transfer. While Coulomb energy transfer is dominated by “long-range” dipole-dipole interactions which cause perturbations of the electronic systems, electron- exchange energy transfer requires much closer contact between *M** and *Q* since it involves an electron transfer mechanism.

The general energy transfer mechanisms described above give different possibilities for the energy transfer process which can be classified according to the initial spin multiplicity M* and the final multiplicity of *Q* (The spin multiplicity is defined as 2*S*+1, where *S* is the overall spin quantum number):

$^1M^* + {}^1Q \rightarrow {}^1M + {}^1Q^*$ singlet-singlet
$^3\mathbf{M}^* + {}^1Q \rightarrow {}^1M + {}^3Q^*$ triplet-triplet
$^3M^* + {}^1Q \rightarrow {}^1M + {}^1Q^*$ triplet-singlet
$^1M^* + {}^1Q \rightarrow {}^1M + {}^3Q^*$ singlet-triplet

Of these four possibilities, the first three are relatively common and the last quite rare. As we will see below there are spin selection rules for each of the different types of energy transfer mechanism.

Radiative energy transfer

Radiative energy transfer involves the emission of a photon from the initially excited molecule *M** and its re-absorption by the molecule *Q*. The two requirements are a good overlap between the emission spectrum of M and efficient absorption of photons emitted from *M** by *Q*. For organic molecules *Q* the $S_o \rightarrow T_1$ absorption spectrum is likely to be weak (spin-forbidden transition), the dominant transfer processes are:

$^1M^* \rightarrow {}^1M + h\nu$	$^1Q + h\nu \rightarrow {}^1Q^*$	singlet-singlet
$^3M^* \rightarrow {}^1M + h\nu'$	$^1Q + h\nu' \rightarrow {}^1Q^*$	triplet-singlet

If the emission spectrum of $^{1,3}M^*$ is denoted by the normalized distribution $F_M(\bar{\upsilon})$, where $\bar{\upsilon}$ represents the wavenumber, and the absorption spectrum of ^1Q is written in terms of $\epsilon_Q(\bar{\upsilon})$ then the probability of radiative energy transfer is given approximately by:

$$P_{RT} = \int_0^\infty F_M(\bar{\upsilon}) \left(1 - 10^{-\epsilon_Q(\bar{\upsilon})[\,^1Q]d}\right) d\bar{\upsilon}$$

where $[^1Q]$ is the concentration of Q in its ground state.

Using the Taylor series expansion $10^{-x} = e^{-2.3026x} = 1 - 2.3026x + \cdots$ we obtain for small values of x:

$$P_{RT} = 2.303\left[\,^1Q\right]d \int_0^\infty F_M(\bar{\upsilon})\epsilon_Q(\bar{\upsilon})d\bar{\upsilon} \quad \text{with} \quad \int_0^\infty F_M(\bar{\upsilon})d\bar{\upsilon} = 1$$

The integral represents the overlap between the donor (M) emission quantum spectrum and the absorption spectrum of the acceptor Q:

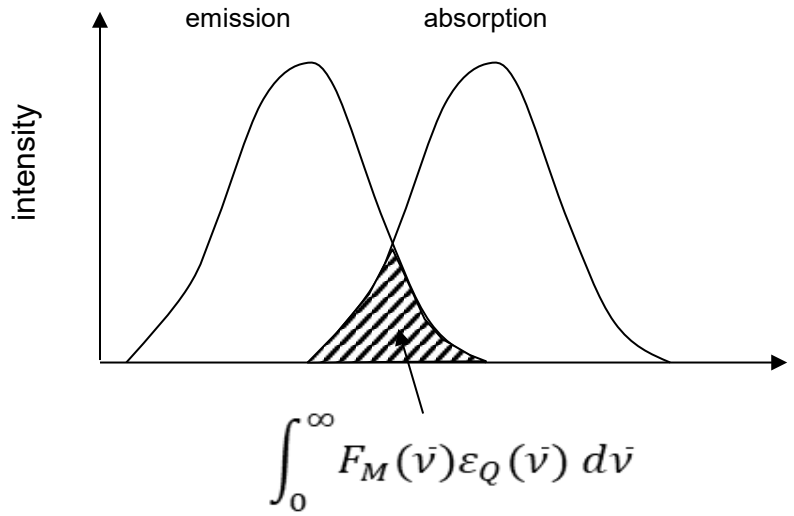

Nonradiative energy transfer

Unlike radiative energy transfer, which requires no specific interaction between energy donor and acceptor, nonradiative mechanisms involve the mutual perturbation of the electronic structures of *M** and *Q*. The process of nonradiative energy transfer may be thought of as a nonradiative transition of a single (*M***Q*) "supermolecule" and much of the theoretical analysis will be treated in this sense.

The rate of nonradiative energy transfer from some state described by the initial state wavefunction ψ_m^M in the (*M***Q*) supermolecule to a final state described by the wavefunction ψ_n^Q is determined by Fermi's golden rule:

$$\frac{d}{dt}P_n = \frac{2\pi}{\hbar}|H_{nm}|^2\bar{\rho}_n$$

where the matrix element H_{nm} now refers to the initial state wavefunction ψ_m^M and the final state wavefunction ψ_n^Q, and $\bar{\rho}_n$ refers to the density of final vibronic (acceptor) states. If a single electronic state in *Q* is involved in the transition, then $\bar{\rho}_n$ will be the density of vibrational states in that electronic state.

Applying the Born-Oppenheimer approximation, H_{nm} can be factorized into an electronic matrix element and a vibrational overlap integral:

$$|H_{nm}| = \langle\psi_n^Q|\hat{H}'|\psi_m^M\rangle = \langle\varphi_n^Q|\hat{H}'|\varphi_m^M\rangle\langle N_n^Q|N_m^M\rangle$$

Where $\hat{H}'$ is the interaction Hamiltonian responsible for the energy transfer process and $|\varphi\rangle$ and $|N\rangle$ are the electronic and nuclear wavefunctions, respectively.

If we assume that the electronic matrix elements $\beta_e = \langle \varphi_n^Q | \hat{H}' | \varphi_m^M \rangle$ do not vary markedly for different pairs of m, n vibronic levels, then an overall nonradiative rate can be defined as follows:

$$\frac{d}{dt} P_n = \frac{2\pi}{\hbar} {\beta_e}^2 \sum_{n,m} \left| \langle N_n^Q | N_m^M \rangle \right|^2 \bar{\rho}_n$$

The last term is the sum of the modulus squared of the vibrational overlap integral multiplied by the density of vibrational levels in the acceptor. This term is related to the spectral overlap integral, such that:

$$\frac{d}{dt} P_n = \frac{2\pi}{\hbar} {\beta_e}^2 \int_0^\infty F_M(\bar{\upsilon}) \epsilon_Q(\bar{\upsilon}) d\bar{\upsilon}$$

This equation is quite general, since it does not include the precise type of energy transfer involved. This information is given by the interaction Hamiltonian $\hat{H}'$ and hence by the electronic matrix element, β_e.

Long-range Coulomb energy transfer

When two molecules come close enough that the electric field of the donor p-electrons can be felt by the p-electrons of the acceptor, the two p-systems are coupled by Coulomb interaction. A classical analogy can be given by a system of coupled springs. The oscillation of the first spring can transfer its energy to the second spring. If the two springs are identical, energy goes back and forth between the two springs. Coming back to the two π-electron systems, energy would be transferred from one molecule to the other, meaning that the donor molecule makes a transition to the ground state while the acceptor molecule is brought to its excited state and so forth. If the energy levels of donor and acceptor are dissimilar, the transfer occurs from the excited donor in its vibrational ground state (Kasha's rule) to the acceptor in a vibrationally excited state. Very rapidly, the acceptor relaxes into its vibrational ground state making the back transfer of energy (from the acceptor to the donor) very improbable. The interaction between the π-electron systems can be approximated by a dipole-dipole interaction. In this case the electronic coupling matrix element becomes:

$$\beta_e = \frac{\vec{\mu}_M \vec{\mu}_Q}{r^3}$$

where $\vec{\mu}_M$ and $\vec{\mu}_Q$ are the transition dipole moments corresponding to the M→M* and Q→Q* transition, and *r* is the distance between them. Förster (1948) demonstrated that the rate constant for weak coupling dipole-dipole energy transfer from M* to Q is given by the expression:

$$k_F = \frac{d}{dt} P_n = \frac{0.529\kappa^2 \phi_{PL}}{n^4 N_A r^6 \tau_M} \int_0^\infty F_M(\bar{v}) \epsilon_Q(\bar{v}) \frac{d\bar{v}}{\bar{v}^4} d\bar{v} \quad \text{with } \kappa = cos\theta_{MQ} 3cos\theta_M \theta_Q \text{ (for in-plane vectors } \vec{\mu}_M, \vec{\mu}_Q).$$

where θ_{MQ} is the angle between the transition dipole moment vectors $\vec{\mu}_M$ and $\vec{\mu}_Q$, θ_M and θ_Q are the angles between $\vec{\mu}_M$and $\vec{\mu}_Q$ and the internuclear M-Q axis, respectively. Furthermore, *n* is the solvent refractive index, N_A is Avogadro's constant and τ_M and ϕ_{PL} is the radiative lifetime of *M** photoluminescence quantum yield, and the numerical value of 0.529 has the units cm. Dipole-dipole energy transfer is also called **Förster energy transfer** and does not involve any electron transfer between donor and acceptor. $\kappa^2 = 2/3$ for randomly oriented dipole vectors $\vec{\mu}_M$ and $\vec{\mu}_Q$.

$$k_F = \frac{d}{dt} P_n = \frac{0.529\kappa^2 \phi_{PL}}{n^4 N_A r^6 \tau_M} \int_0^\infty F_M(\bar{\upsilon}) \epsilon_Q(\bar{\upsilon}) \frac{1}{\bar{\upsilon}^4} d\bar{\upsilon} \qquad \text{with } \kappa = cos\theta_{MQ} - 3cos\theta_M \theta_Q \text{ (for in-plane vectors } \vec{\mu}_M, \vec{\mu}_Q)$$

where θ_{MQ} is the angle between the transition dipole moment vectors $\vec{\mu}_M$ and $\vec{\mu}_Q$, θ_M and θ_Q are the angles between $\vec{\mu}_M$and $\vec{\mu}_Q$ and the internuclear M-Q axis, respectively. Furthermore, *n* is the solvent refractive index, N_A is Avogadro's constant and τ_M and ϕ_{PL} is the radiative lifetime of *M** photoluminescence quantum yield, and the numerical value of 0.529 has the units cm. Dipole-dipole energy transfer is also called **Förster resonance energy transfer (FRET)** and does not involve any electron transfer between donor and acceptor.

Defining a critical transfer distance r_o as the M-Q separation at which $^d/_{dt}\ P_n = {}^1/_{\tau_M}$, where τ_M is the actual donor excited state lifetime in the absence of *Q*, r_o is given by:

$$r_0^6 = \frac{0.529\kappa^2 \phi_{PL}}{n^4 N_A} \int_0^\infty F_M(\bar{\upsilon}) \epsilon_Q(\bar{\upsilon}) \frac{d\bar{\upsilon}}{\bar{\upsilon}^4}$$

In terms of r_o, the Förster rate is often expressed as: $k_F = \frac{1}{\tau_M} \frac{r_0^6}{r^6}$. The FRET efficiency is given as:

$$E_{FRET} = \frac{k_F}{k_F + k_M} = \frac{1}{1 + \frac{r^6}{r_0^6}}$$

FRET Pair	ϕ_D [a]	ε_A ($mM^{-2} \cdot cm^{-1}$) [b]	r_0 (nm) [c]	Reference
ECFP-EYFP	0.4	83	4.9	[75]
mTurquoise2-sEYFP	0.93	101	5.9	[2]
mTurquoise2-mVenus	0.93	92	5.8	[35]
EGFP-mCherry	0.6	72	5.4	[2]
Clover-mRuby2	0.76	113	6.3	[2]
mClover3-mRuby3	0.78	128	6.5	[45]
mNeonGreen-mRuby3	0.8	128	6.5	[45]
eqFP650-iRFP	0.24	105	5.8	this work [e]
mAmetrine-tdTomato [d]	0.58	138	6.6	this work [e]
LSSmOrange-mKate2 [d]	0.45	63	7.0	this work [e]
EGFP-sREACh	0.6	115	5.8	[64]
EGFP-ShadowG	0.6	89	4.7	[64]
EGFP-activated PA-GFP	0.6	17	4.4	this work [e]
EGFP-Phanta	0.6	98	5.8	this work [e]
mTagBFP-sfGFP	0.63	83	4.6	this work [e]
mVenus-mKOκ	0.57	105	6.3	this work [e]
CyOFP1-mCardinal [d]	0.76	87	6.9	this work [e]

D....donor
A....acceptor

Since the transfer mechanism is a long range Coulombic interaction, there is no need to form an intermediate complex (or encounter pair) for energy transfer to occur. The electron spin restrictions that apply are therefore those that apply to the molecules individually, i.e. no change in the overall spin of either M or Q is allowed. The favored energy transfer processes are therefore:

$^1M^* + {}^1Q \rightarrow {}^1M + {}^1Q^*$
$^1M^* + {}^3Q \rightarrow {}^1M + {}^3Q^*$

The latter process involves the transfer of energy to a triplet state of Q. If Q has a singlet ground state, ^3Q will represent the first electronically excited triplet state T_1, and so energy transfer will yield a higher triplet state T_2.

FRET techniques – a nanoruler for biosensing and imaging

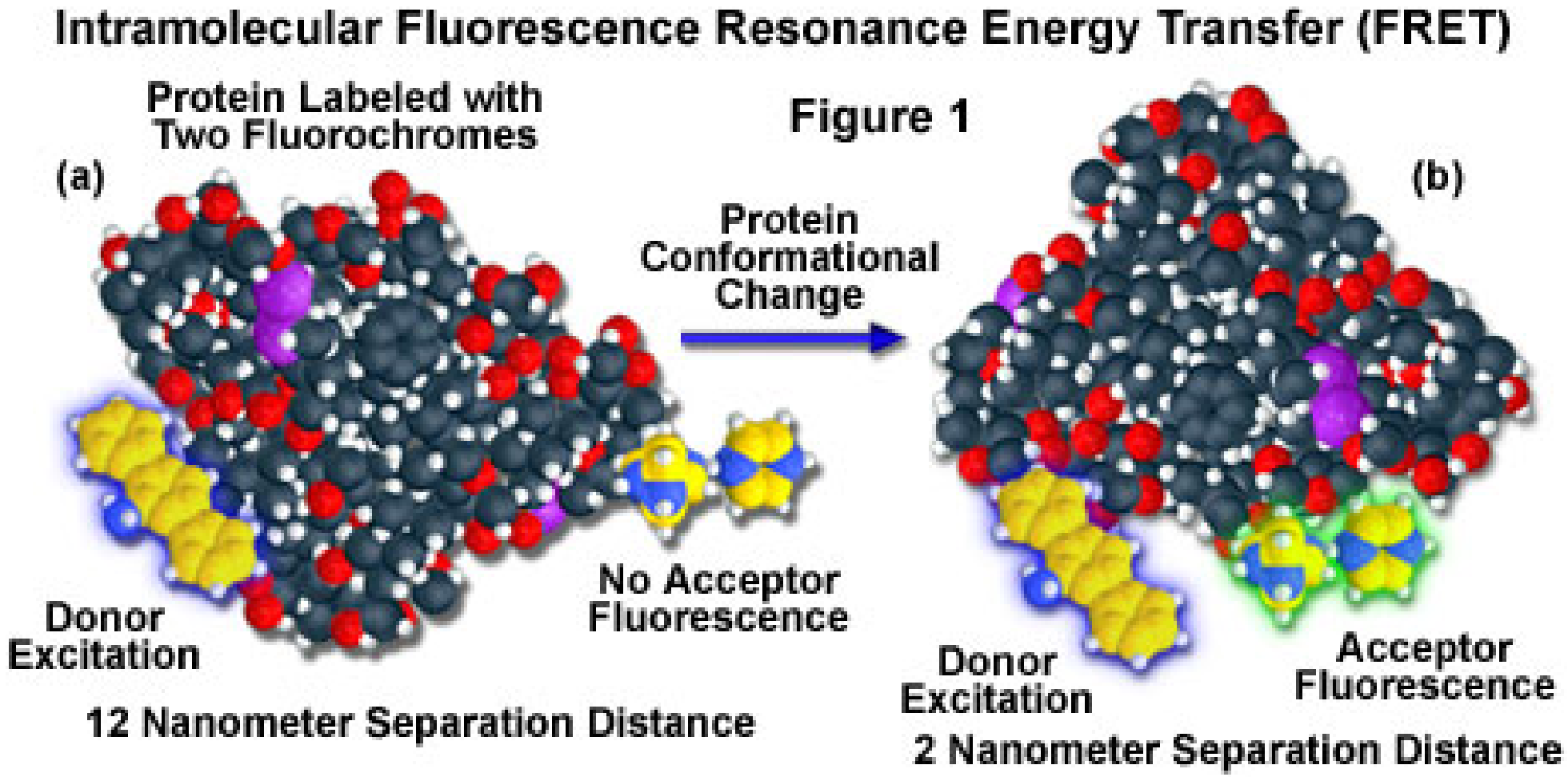

Short range electron-exchange energy transfer

Intermolecular electron exchange is considered to be the dominant interaction responsible for energy transfer in situations where molecules are very close together (3 to 5 Å). Unlike the Coulombic exchange mechanism, energy transfer by electron-exchange requires the physical transfer of electrons between donor and acceptor. Indeed, it is useful to think of electron-exchange energy transfer proceeding via the formation of a short-lived intermediate pair. Dexter expressed a weak coupling exchange-transfer rate constant in terms of Z^2, which cannot be directly related to optical experiments, and a spectral overlap integral, which replaces the vibrational overlap and the density of states. The transfer rate constant for a single M*-Q pair may be written as:

$$\frac{d}{dt}P_n = \frac{2\pi}{\hbar}Z^2 \int_0^\infty F_M(\bar{\nu})\varepsilon_Q(\bar{\nu})\, d\bar{\nu}$$

Dexter (1953) found that:

$$Z^2 \propto e^{-2r/l}$$

Where r is the distance between donor and acceptor molecules and l is the van der Waals radius of the donor-acceptor pair (sum of the van der Waals radii of donor and acceptor molecules). The exponential decay of Z comes from the fact that Z depends on the intermolecular orbital overlap and that molecular wavefunctions decline approximately exponentially at large r. Again we can look for a critical radius below which **Dexter energy transfer** is effective. Typical values are < 10 Å. Note that Z^2 is independent of factors which determine the strengths of the M*→M and Q→Q* transitions.

Now that a "precursor pair" is formed between M and Q before energy transfer, restrictions on electron spin changes are determined by the spin of the *complex* which is formed. According to the **Wigner spin rule**, the total spin S_r of the complex which is formed from two molecules with spins S_1 and S_2 may take the values:

$$S_r = S_1 + S_2, S_1 + S_2 - 1, \ldots, |S_1 - S_2|$$

If the products of the energy transfer reaction possess spins S_3 and S_4, the latter combine to produce the total spin S_r as above:

$$S_r = S_3 + S_4, S_3 + S_4 - 1, \ldots, |S_3 - S_4|$$

According to the spin conservation rule, if and only if the two series S_r above contain at least one common element, then the short range energy transfer is spin allowed.

The interaction of $^1M^*$ and ^1Q may give rise to a complex with $S_r = 0$. There is therefore one spin-allowed energy transfer reaction:

$^1M^* + {}^1Q \rightarrow {}^1M + {}^1Q^*$ singlet-singlet

This reaction is also allowed by Förster energy transfer. A singlet-triplet reaction ($^1M^* + {}^1Q \rightarrow {}^1M + {}^3Q^*$) would yield the value $S_r = 1$ for the product pair which does not correspond to the spin of the reactant pair. The singlet-triplet reaction is also forbidden in Förster transfer. In special cases, where intersystem crossing is enhanced by heavy atoms this rare reaction can nevertheless be observed.

Further allowed reactions from the triplet excited state $^3M^*$ are:

$^3M^* + {}^1Q \rightarrow {}^1M + {}^3Q^*$ triplet-triplet
$^3M^* + {}^3Q \rightarrow {}^1M + {}^1Q^*$ triplet-singlet

The first occurs via a complex with $S_r = 1$, which corresponds to the product complex with $S_r = 1$. The second reaction has reactant pair of $S_r = 2$, 1 or 0 and is therefore compatible with several product complex spins, such as $S_r = 0$. Both reaction are forbidden for the Coulomb mechanism.

There are not many organic molecules with a triplet ground state. Molecular oxygen is the commonest candidate for ^3Q. Oxygen is also an effective quencher of singlet excited states via the formation of a triplet exciplex $^3(MO_2)^{**}$. Therefore, all the studies of the photophysics of excited molecules are best done in the absence of oxygen.

In natural photosynthesis, energy transfer reactions play an important role. In photochemistry, an important application of the energy transfer theory is triplet-triplet energy transfer and sensitization.

We have seen that it is generally very difficult to get high concentrations of organic molecules in the triplet excited state. This is because most of the molecules have paired electrons in the ground state and are therefore singlet states (the singlet-triplet optical transition is spin forbidden). There is one group of molecules containing carbonyl substituents which efficiently produce triplet states by absorption of light. The molecule benzophenone (or diphenylketone) can be excited to the singlet state (S_1) from n→p* transition. As for other aromatic ketones, intersystem crossing to the triplet state T_1 is very rapid and occurs with a quantum efficiency of nearly unity. This allows to reach an important population of excited triplet states of benzophenone and according to the triplet-triplet energy transfer reaction ($^3M^* + {}^1Q \rightarrow {}^1M + {}^3Q^*$) this triplet excited state can be transferred to an acceptor. This process is also termed as "sensitization".

As an example, the energetics in the case of the couple benzophenone-naphthalene is shown:

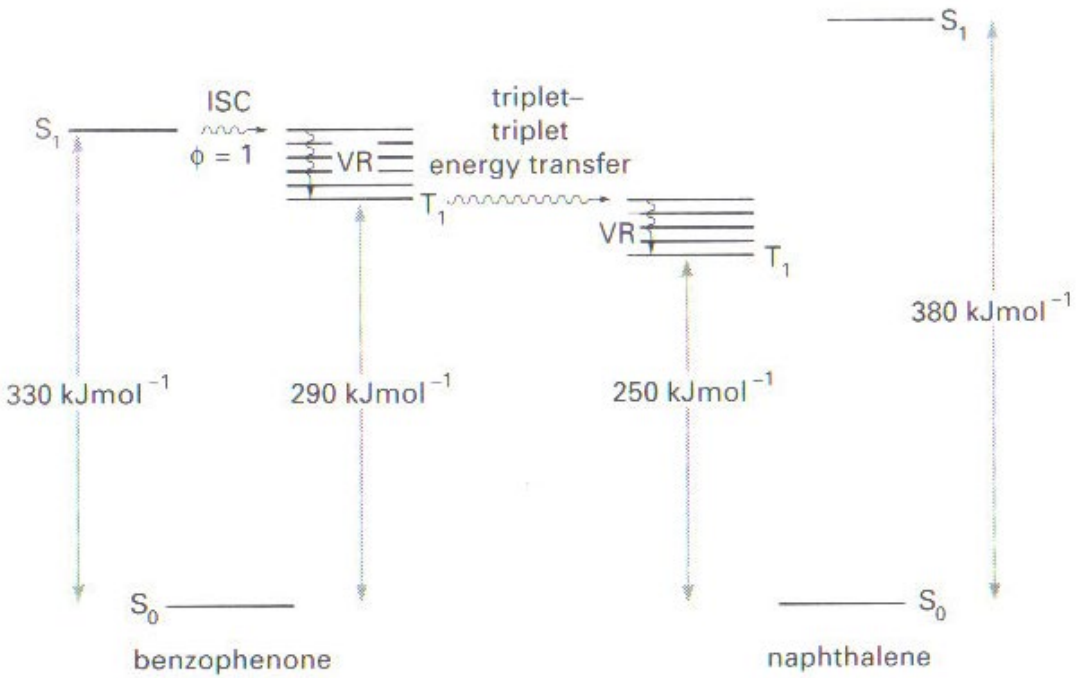

This kind of reaction is quite important for photochemistry, since it allows to study reactions from the triplet excited state, which are often quite different from reactions occurring from the singlet excited state.

Various interaction in the solid state

Van der Waals interaction:

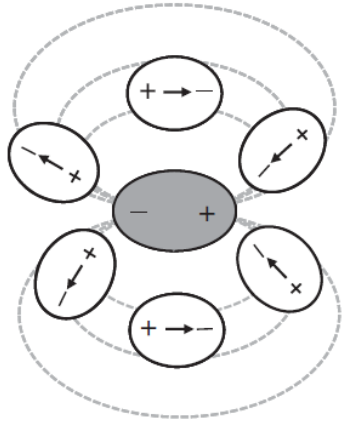

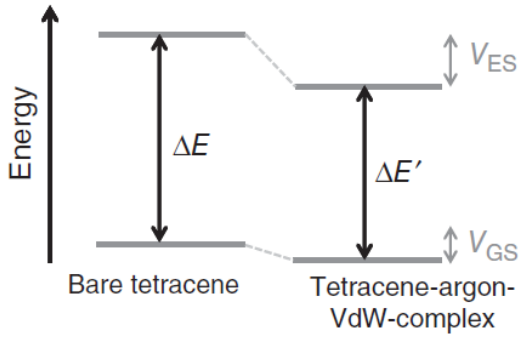

electron coupling β and carrier mobility:

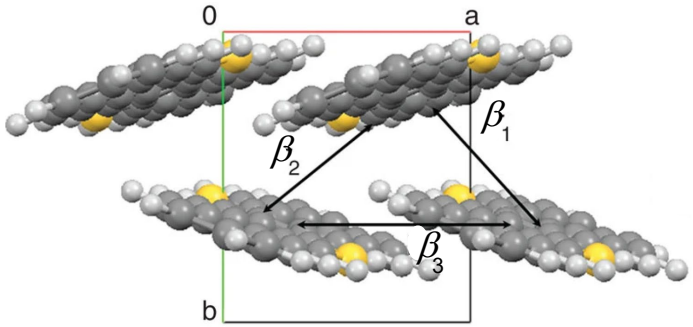

exciton coupling J:

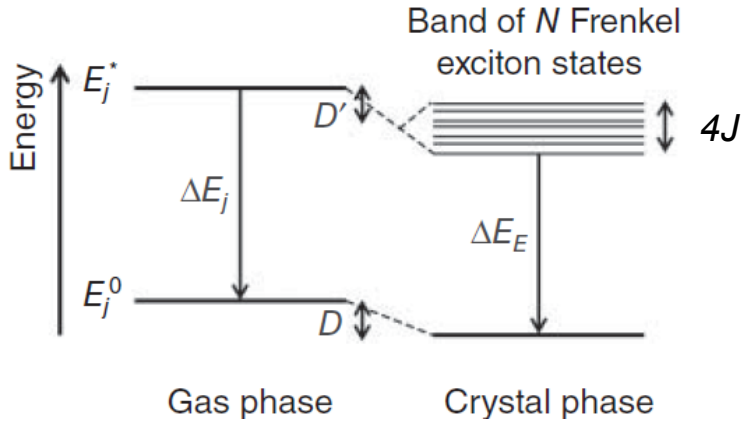

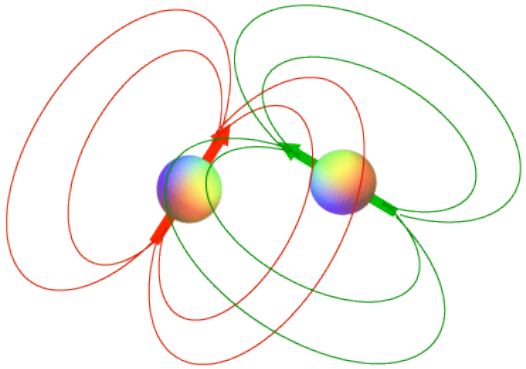

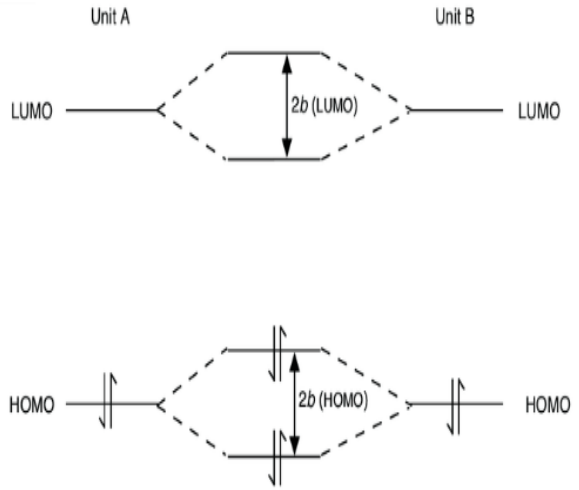

A. Köhler and H. Bässler *Electronic Processes in Organic Semiconductors*

Four different crystalline structures of a merocyanine dye

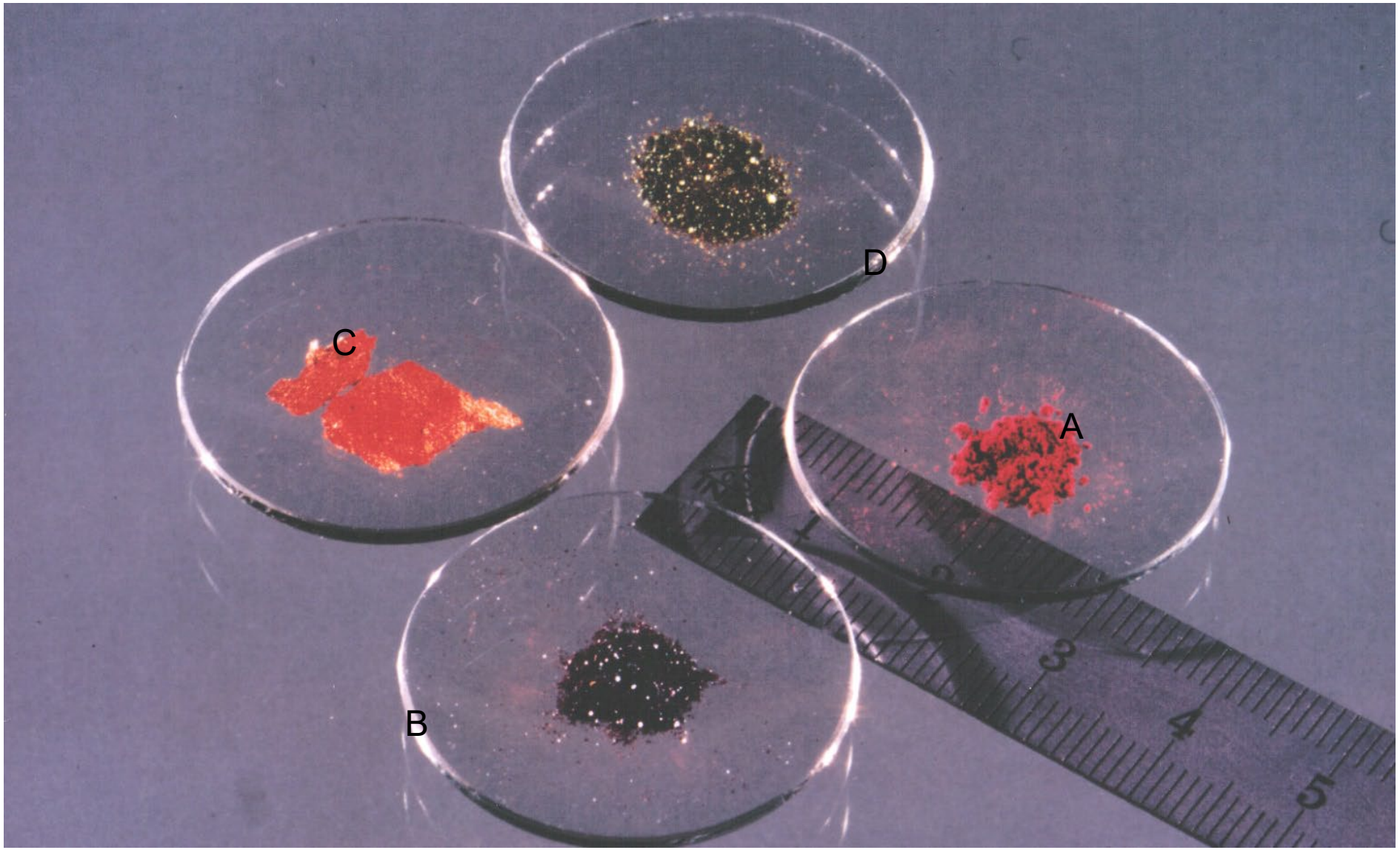

Fullerene C_{60}

In 1985, a new allotropic form of carbon with the molecular formula C_{60} was discovered (Kroto et al.). It is called buckminsterfullerene named after the architect R. Buckminster Fuller, who designed spherical architectural structures composed of polygons. C_{60} behaves as a typical molecular solid like anthracene, which is an insulator, but it also forms compounds that are metallic and even superconducting. Furthermore it is an excellent electron acceptor, making it an invaluable component for organic photovoltaics.

The crystalline structure of fullerene is face-centered cubic (lattice constant of 14.17 Å) giving rise to tetrahedral as well as octahedral sites within the crystal lattice. Many of the solid C_{60} properties are largely given by the individual molecular properties. For example, there is practically no difference in the position of the absorption peaks in solution and in the solid, pointing up the weak molecular nature of the bonding in the solid.

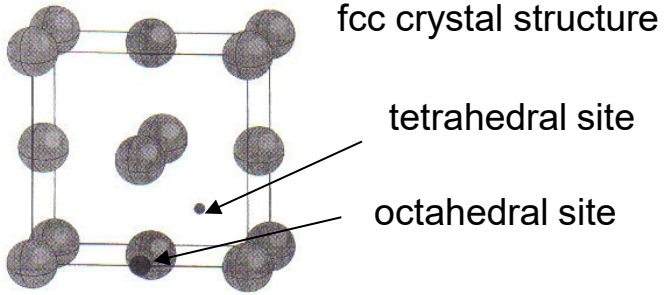

stereoscopic view of C_{60}

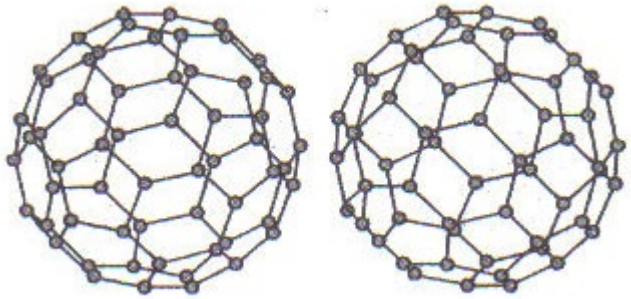

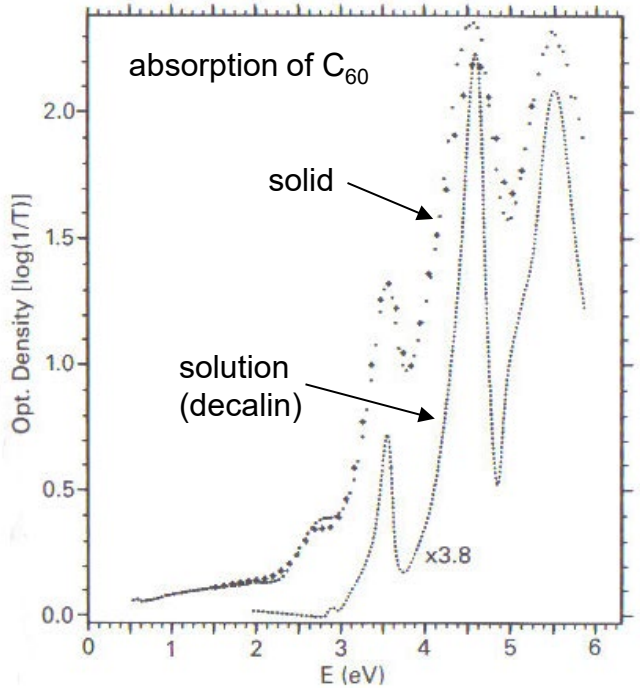

Molecular exciton theory –transfer of energy

monomer

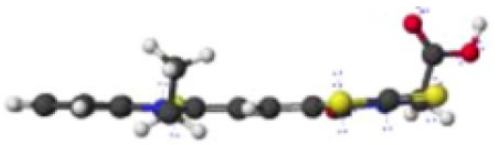

$$M + M \overset{K}{\rightleftharpoons} D$$

$$K = \frac{[D]}{[M]^2}$$

equilibrium constant K

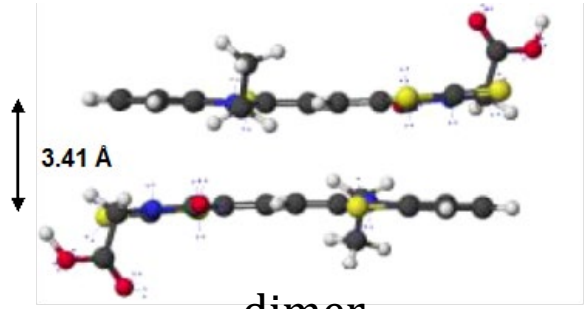

dimer

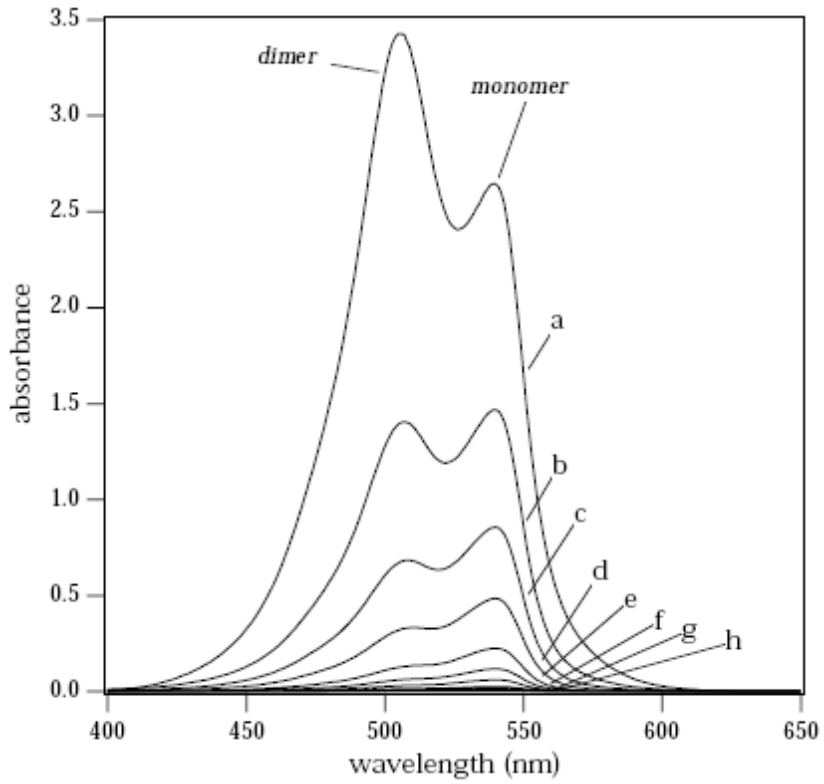

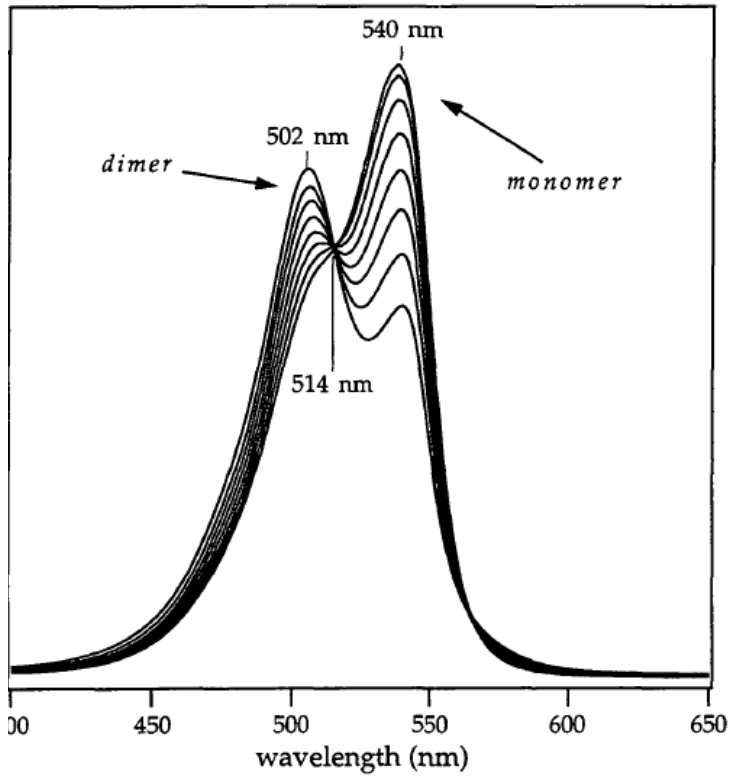

Absorption spectrum of a merocyanine dye in water for different concentrations. a: $5 \cdot 10^{-4}$ M, b: $2 \cdot 10^{-4}$ M, c: $1 \cdot 10^{-4}$ M, d: $5 \cdot 10^{-5}$ M, e: $2 \cdot 10^{-5}$ M, f: $1 \cdot 10^{-6}$ M , g: $5 \cdot 10^{-6}$ M, h: $2 \cdot 10^{-6}$ M.

F. Nüesch et al., Chemical Physics 193 (1995) 1-17

Localized vs delocalized excitons in semiconductors

Due to the low dielectric constant in organic semiconductors (ε = 3-4) holes and electrons are not screened as much as in inorganic semiconductors (ε = 10-15). Also the electronic wavefunctions are localized as compared to those in inorganic semiconductors.

These conditions lead to high binding energy for excitons in organic semiconductors of about 0.4 eV, which means that excitons can not thermally be separated into free charge carriers. This contrasts with inorganic semiconductors, where excitons can be thermally split into free charge carriers at room temperature.
A large enough driving force (at least as high as the exciton binding energy) is therefore required for charge separation in organic semiconductors (strong electric field, heterointerface).

While delocalized **Wannier-Mott excitons** can be treated similar to a hydrogen atom to understand their optical properties, for **localized Frenkel excitons** in organic semiconductors and silver halides, a different treatment is required.

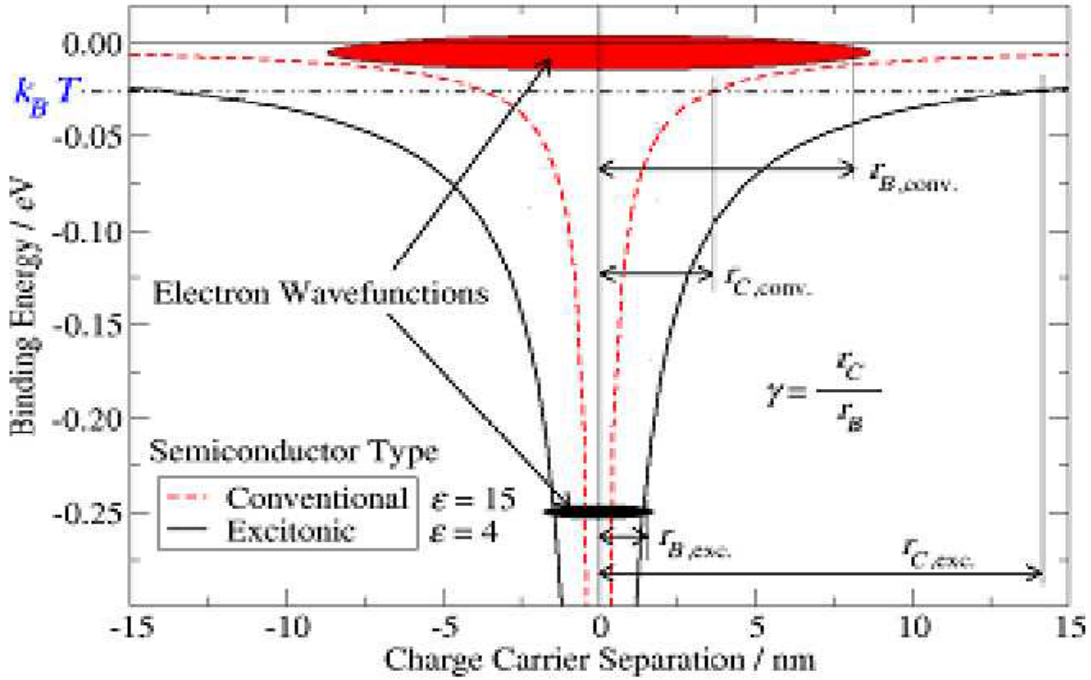

Adapted from Brian A. Gregg et al., Journal of Applied Physics, 93 (2003) 3605

Energy transfer processes

Energy transfer (ET) is an extremely important process in organic semiconductor devices with huge implications photochemistry, optoelectronics, biochemistry and sensorics. It can be viewed as follows:

$A^* + B \overset{ET}{\Rightarrow} A + B^*$ *A* and *B* designate the ground states of the molecules, A^* and B^* stand for the excited states.

The different processes may be classified according to:

- Radiative energy transfer in which the emitted photon from A^* is reabsorbed by B:
  This process requires that the emission spectrum of A^* overlaps with the absorption spectrum of B
.
- Nonradiative energy transfer in which a specific interaction between A^* and *B* is required. Two types of interaction may be identified which are termed Coulomb and electron-exchange energy transfer.

Coulomb energy transfer is dominated by “long-range” dipole-dipole interactions which cause perturbations of the electronic systems. It is also called **Förster Resonance Energy Transfer** (FRET) and has a range of 1-10 nm.

Electron exchange energy transfer, also called **Dexter Energy Transfer**, requires much closer contact between A^* and *B* since it involves an electron transfer mechanism. The typical range is 3-10 Å.

Molecular excitons

The formation of new absorption bands induced by intermolecular energy transfer interaction was considered by A. S. Davydov in 1948. Here we will treat the problem in a simpler way such as developed by Mc Rae and Kasha in 1964. The essential assumption of the theory is that the interaction between two p-systems A and B upon absorption of a photon relies on energy resonance:

$$A^* + B \overset{ET}{\Leftrightarrow} A + B^*$$

A* and B* denote the excited states of the molecules A and B.

Assuming a weak interaction, i.e. a small overlap between the molecular orbitals allows to treat the problem as a small perturbation:

$$\hat{H} = \hat{H}_A + \hat{H}_B + V_{AB}$$

Where $\hat{H}$ is the total Hamiltonian of the dimer, $\hat{H}_A$ and $\hat{H}_B$ are the Hamiltonians of molecules A and B and V_{AB} is the interaction potential between the two molecules. The latter term corresponds the the Coulomb interaction between electrical charges: $V_{AB} = e^2/r$.

The task is now to solve the Schrödinger equation for the Hamiltonian $\hat{H}$. The following Ansatz is made for the ground state wave function:

$\phi_G = \psi_A \psi_B$ where ψ_A and ψ_B are Eigenfunctions of molecules A and B with energy *E*.

(the ground state is written as a product of molecular wavefunctions, since we are precisely looking at the interaction between them).

For the ground state energy one obtains:

$$E_G = \langle \phi_G | \hat{H} | \phi_G \rangle = \langle \phi_G | \hat{H}_A + \hat{H}_B + V_{AB} | \phi_G \rangle = 2E + \underbrace{\langle \phi_G | V_{AB} | \phi_G \rangle}_{W' < 0 \ (v.d.Walls)}$$

For the excited state wave function the assumption of energy resonance leads to:

$$\phi_{E'} = r\tilde{\psi}_A \psi_B + s\psi_A \tilde{\psi}_B$$

where $\tilde{\psi}_A$ is the excited state wave function of A with energy $\tilde{E}$ and $\tilde{\psi}_B$ is the excited state wave function of molecule B with energy $\tilde{E}$. For the energy in the excited state one can write:

$$E' = \frac{\langle \phi_{E'} | \hat{H} | \phi_{E'} \rangle}{\langle \phi_{E'} | \phi_{E'} \rangle} = \frac{\langle r\tilde{\psi}_A \psi_B + s\psi_A \tilde{\psi}_B | \hat{H}_A + \hat{H}_B + V_{AB} | r\tilde{\psi}_A \psi_B + s\psi_A \tilde{\psi}_B \rangle}{\langle r\tilde{\psi}_A \psi_B + s\psi_A \tilde{\psi}_B | r\tilde{\psi}_A \psi_B + s\psi_A \tilde{\psi}_B \rangle} = \frac{f(r,s)}{g(r,s)}$$

$$\Rightarrow \frac{dE'}{dr} = 0 \quad \text{and} \quad \frac{dE'}{ds} = 0 \quad \text{and therefore} \ \frac{dE'}{dr} = \frac{f'g - fg'}{g^2} = 0 \ \text{and} \ f' - E'g' = 0$$

Before carrying out the derivation, we simplify the terms f and g:

$$f = \langle r\tilde{\psi}_A\psi_B + s\psi_A\tilde{\psi}_B|\hat{H}|r\tilde{\psi}_A\psi_B + s\psi_A\tilde{\psi}_B\rangle = \langle r\tilde{\psi}_A\psi_B + s\psi_A\tilde{\psi}_B|\hat{H}_A + \hat{H}_B + V_{AB}|r\tilde{\psi}_A\psi_B + s\psi_A\tilde{\psi}_B\rangle$$
$$= r^2(\tilde{E} + E) + s^2(\tilde{E} + E) + \langle r\tilde{\psi}_A\psi_B + s\psi_A\tilde{\psi}_B|V_{AB}|r\tilde{\psi}_A\psi_B + s\psi_A\tilde{\psi}_B\rangle$$
$$= r^2(\tilde{E} + E) + s^2(\tilde{E} + E) + r^2\langle\tilde{\psi}_A\psi_B|V_{AB}|\tilde{\psi}_A\psi_B\rangle + s^2\langle\psi_A\tilde{\psi}_B|V_{AB}|\psi_A\tilde{\psi}_B\rangle + 2\mathrm{rs}\langle\tilde{\psi}_A\psi_B|V_{AB}|\psi_A\tilde{\psi}_B\rangle$$

$$g = \langle r\tilde{\psi}_A\psi_B + s\psi_A\tilde{\psi}_B|r\tilde{\psi}_A\psi_B + s\psi_A\tilde{\psi}_B\rangle = r^2 + s^2 + \underbrace{2rs\langle\tilde{\psi}_A\psi_B|\psi_A\tilde{\psi}_B\rangle}_{\approx 0\ (small\ overlap)}$$

For simplification we use

$\langle\tilde{\psi}_A\psi_B|V_{AB}|\tilde{\psi}_A\psi_B\rangle = \langle\psi_A\tilde{\psi}_B|V_{AB}|\psi_A\tilde{\psi}_B\rangle = W''$ (<0, v.d. Waals energy in the excited state)

$\langle\tilde{\psi}_A\psi_B|V_{AB}|\psi_A\tilde{\psi}_B\rangle = \langle\psi_A\tilde{\psi}_B|V_{AB}|\tilde{\psi}_A\psi_B\rangle = J$ (excitonic coupling energy)

We get:

$f = r^2(\tilde{E} + E) + s^2(\tilde{E} + E) + r^2W'' + s^2W'' + 2\mathrm{rs}\,J$
$g = r^2 + s^2$

Calculating $f' - E'g' = 0$ we obtain by taking the derivation with respect to r:

$2r(\tilde{E} + E) + 2rW'' + 2\mathrm{s}\,J - E'2r = 0$ or

$r(\tilde{E} + E + W'' - E') + \mathrm{s}\,J = 0$. In analogy, we can derive with respect to s and obtain:
$\mathrm{r}\,J + s(\tilde{E} + E + W'' - E') = 0$

Nontrivial solutions of this linear homogeneous system of equations for r and s are obtained if:

$$\mathrm{Det}\begin{bmatrix} \tilde{E} + E + W'' - E' & J \\ J & \tilde{E} + E + W'' - E' \end{bmatrix} = 0$$

Solving for the excited state energy of the dimer AB we get:

$$E_+ = \tilde{E} + E + W'' + J$$
$$E_- = \tilde{E} + E + W'' - J$$

and $\quad \phi_{E_{+-}} = \frac{1}{\sqrt{2}}\tilde{\psi}_A\psi_B \pm \frac{1}{\sqrt{2}}\psi_A\tilde{\psi}_B$

Using the point dipole approximation to solve the integral for J one obtains for the exciton coupling energy:

$$J = \frac{1}{4\pi\varepsilon_0\varepsilon}\left[\frac{\vec{\mu}_A\vec{\mu}_B}{r^3} - \frac{3(\vec{\mu}_A\vec{r})\cdot(\vec{\mu}_B\vec{r})}{r^5}\right] \quad \text{with} \quad \vec{\mu}_A = \int \psi_A\vec{\mu}\tilde{\psi}_A \quad \text{and} \quad \vec{\mu}_B = \int \psi_B\vec{\mu}\tilde{\psi}_B$$

$\vec{\mu}_A$ and $\vec{\mu}_B$ are the transition dipole moments of molecule A and B, respectively, ε is the dielectric constant of the surrounding, $\vec{r}$ is the vector connecting the centers of the transition dipole vectors. The exciton coupling energy can be as high as 200 meV for strong transition dipole moments (strong absorbers)

For collinear transition dipole moments of identical molecules a simple expression can be derived:

$$J = \frac{\vec{\mu}^2}{4\pi\varepsilon_0\varepsilon r^3}(1 - cos^2\theta)$$

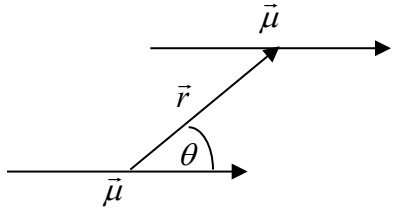

In summary, the interaction between excited states yields to the following energy level shifts for a dimer with parallel transition dipole moments:

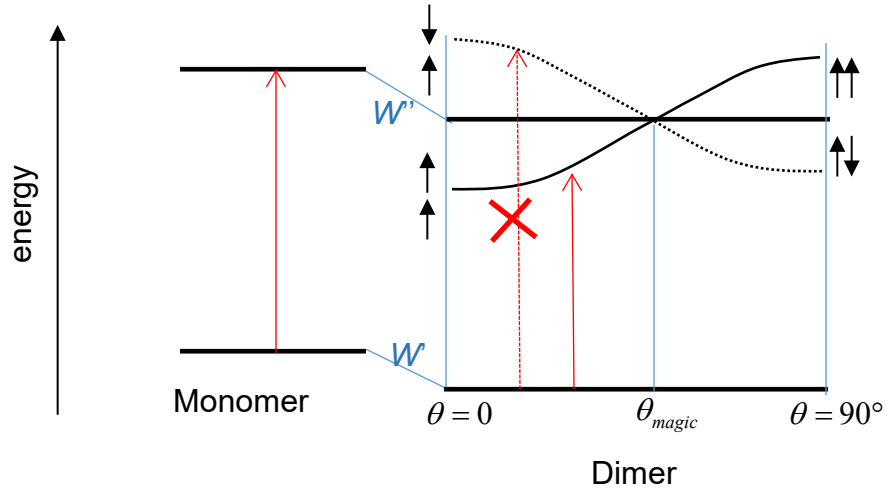

The arrows indicate the symmetric (allowed transition) and anti-symmetric (forbidden transition) coupling of the individual transition dipole moments. A more general description would also allow antiparallel molecular geometries. In this case both transition would be allowed, with distinct polarisations (see figure to the right).

For non-interacting molecules A and B, the transition dipole moment is $\overrightarrow{\mu_A} = \langle \Psi_A | e\vec{r} | \tilde{\Psi}_A \rangle$ and is $\overrightarrow{\mu_B} = \langle \Psi_B | e\vec{r} | \tilde{\Psi}_B \rangle$. Accordingly, the transition dipole moment $\vec{M}$ of the dimer is given by:

$$\vec{M}_{\pm} = \langle \Phi_G | e\vec{r} | \Phi_E \rangle =$$
$$^1/_{\sqrt{2}} \langle (\Psi_A \Psi_B) | e\vec{r} | \Psi_A \tilde{\Psi}_B \pm \tilde{\Psi}_A \Psi_B \rangle =$$
$$^1/_{\sqrt{2}} \langle \Psi_B | e\vec{r} | \tilde{\Psi}_B \rangle \pm {}^1/_{\sqrt{2}} \langle \Psi_A | e\vec{r} | \tilde{\Psi}_A \rangle =$$
$$^1/_{\sqrt{2}} (\vec{\mu}_A \pm \vec{\mu}_B)$$

Therefore for parallel chromophores in the one optical transition is forbidden (see dotted line in left diagram). For non-parallel chromophores in the dimer both transitions are allowed (see below).

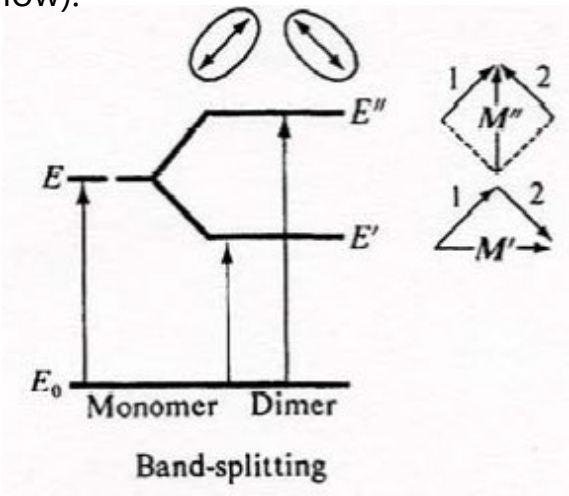

The calculation of spectral shifts using the point dipole approximation is excellent for intermolecular distances of a few nanometers. It can lead to errors (even in the sign of the spectral shift) when it is applied to short intermolecular distances. For short distances, H. Kuhn in 1962 elaborated another model called the extended dipole model. In this model the molecule is represented as a dipole with a positive and negative charge Q separated by a distance l:

The exciton splitting term J (which is equivalent to e) is the given by:

$$J = \frac{Q^2}{4\pi\varepsilon_0\varepsilon}\left(\frac{1}{r_1}+\frac{1}{r_2}-\frac{1}{r_3}-\frac{1}{r_4}\right) \qquad \text{with} \qquad \mu = Q \cdot l$$

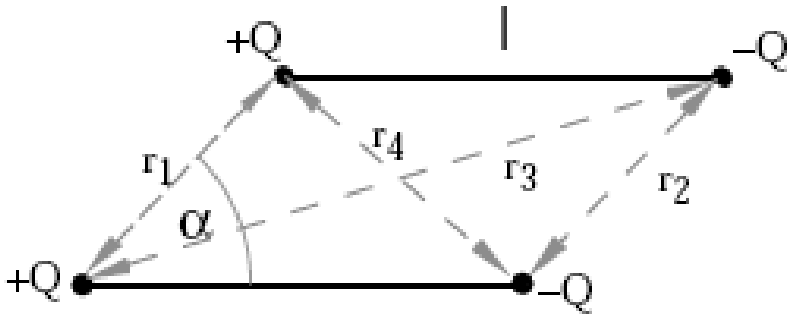

As a final remark it has to be added that exciton theory is not only applicable to the simplest case of a dimer, but that it can be applied to any assembly of molecules. In the case of N molecules, the ground and excited state wavefunctions are:

$$\phi_G = \psi_1\psi_2 \cdot \cdots . \psi_N \qquad \text{and} \qquad \phi_{E'} = \sum_{i=1}^{N} \psi_1\psi_2 \cdot\cdot \tilde{\psi}_i \cdot \ \psi_N$$

Some important results coming out of exciton theory: the exciton coupling energy J determines the splitting of the absorption bands. It is proportional to μ^2 and therefore also to the extinction coefficient. It depends strongly on distance and orientation. In a molecular crystal there are as many exciton bands as there are translationally inequivalent molecules per unit cell. Furthermore, these bands have distinct polarisations.

Weak versus strong exciton coupling in molecular aggregates

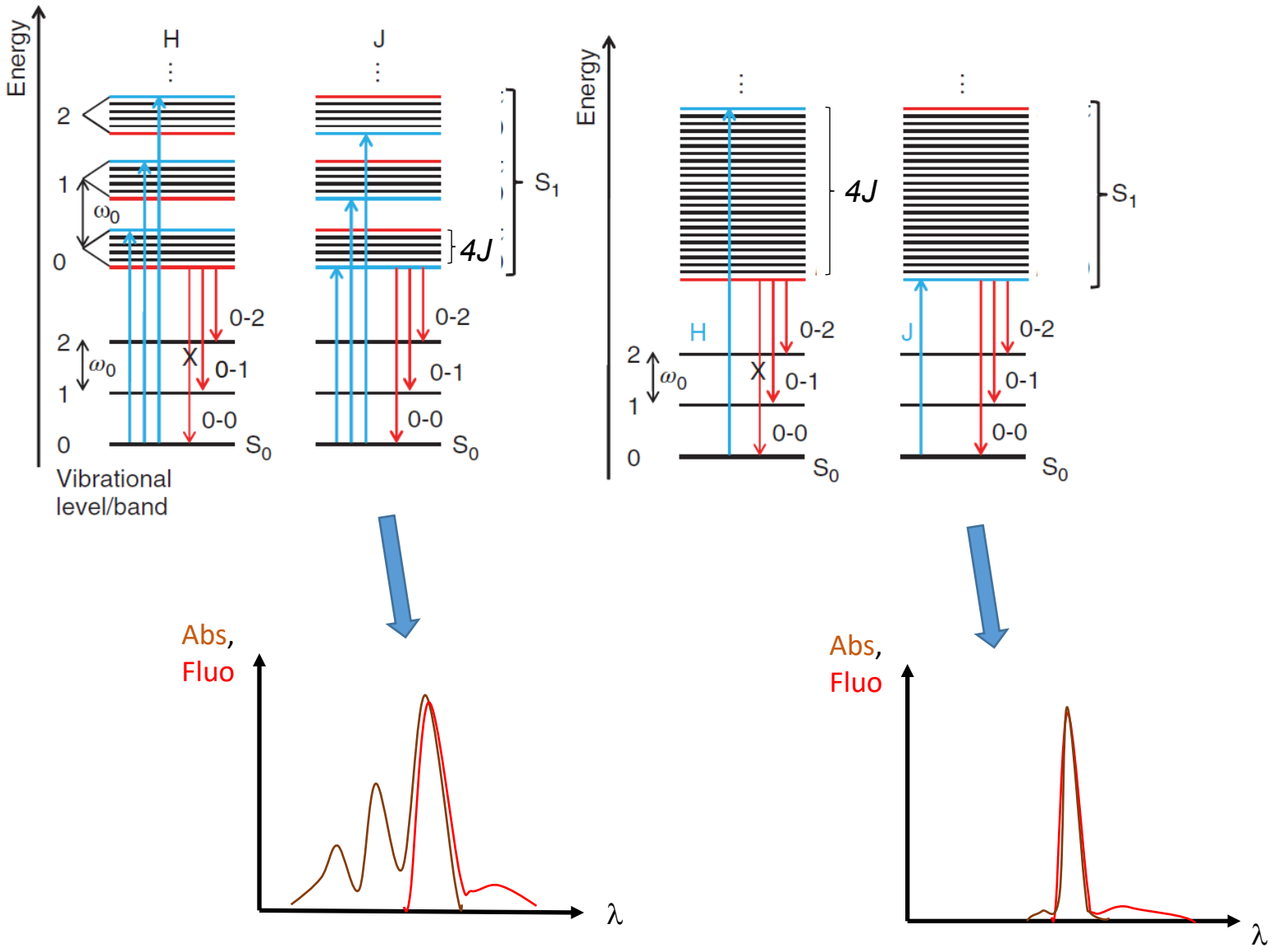

Examples of strongly coupled J- and H-aggregates

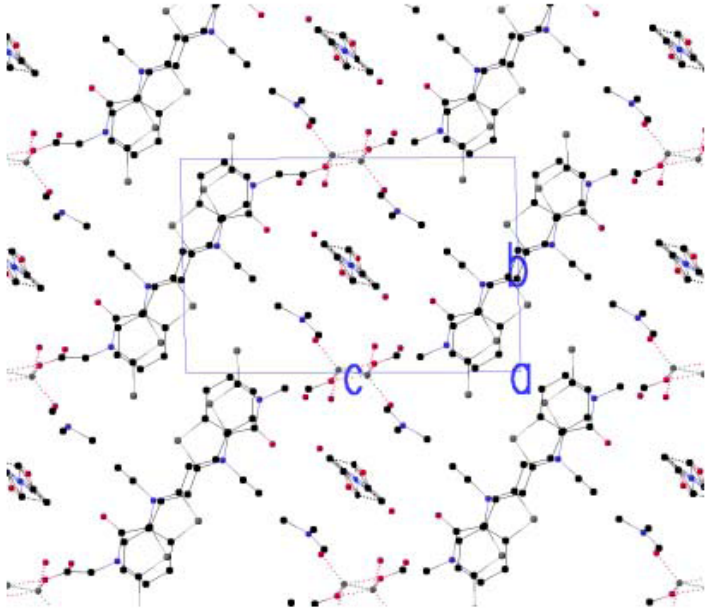

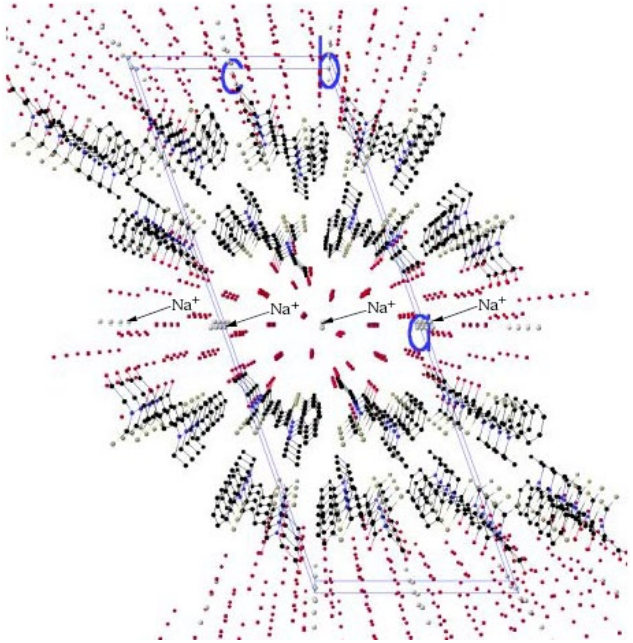

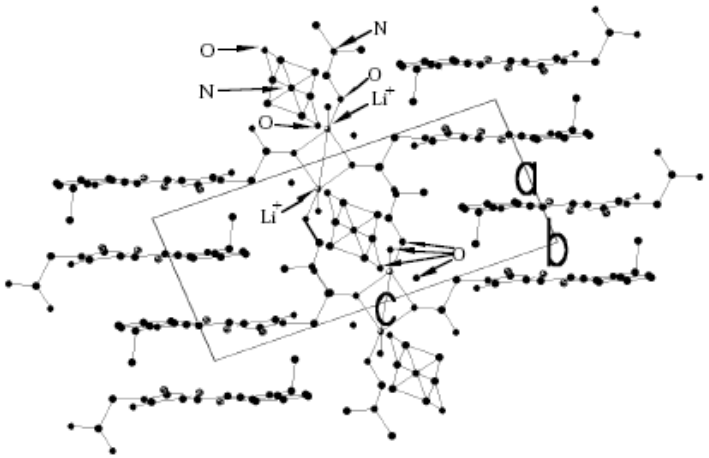

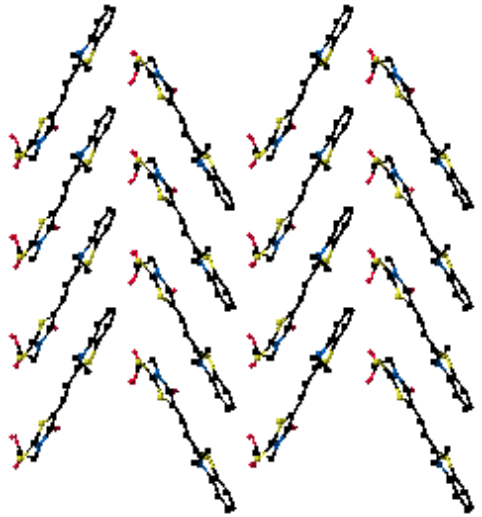

Merocyanine H- and J- aggregates in a porous TiO_2 film as a function of relative humidity (RH)

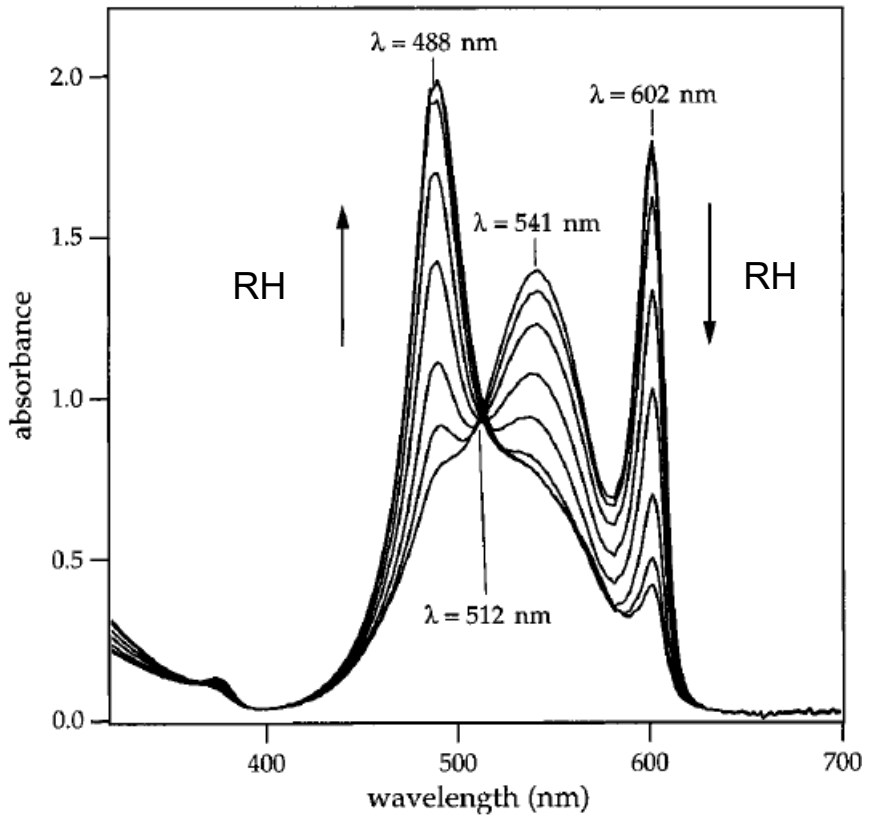

F. Nüesch et al., J. Am. Chem. Soc., Vol. 118, No. 23, (1996) 5420-5431

Beyond the classical picture of Coulomb coupled molecular aggregates

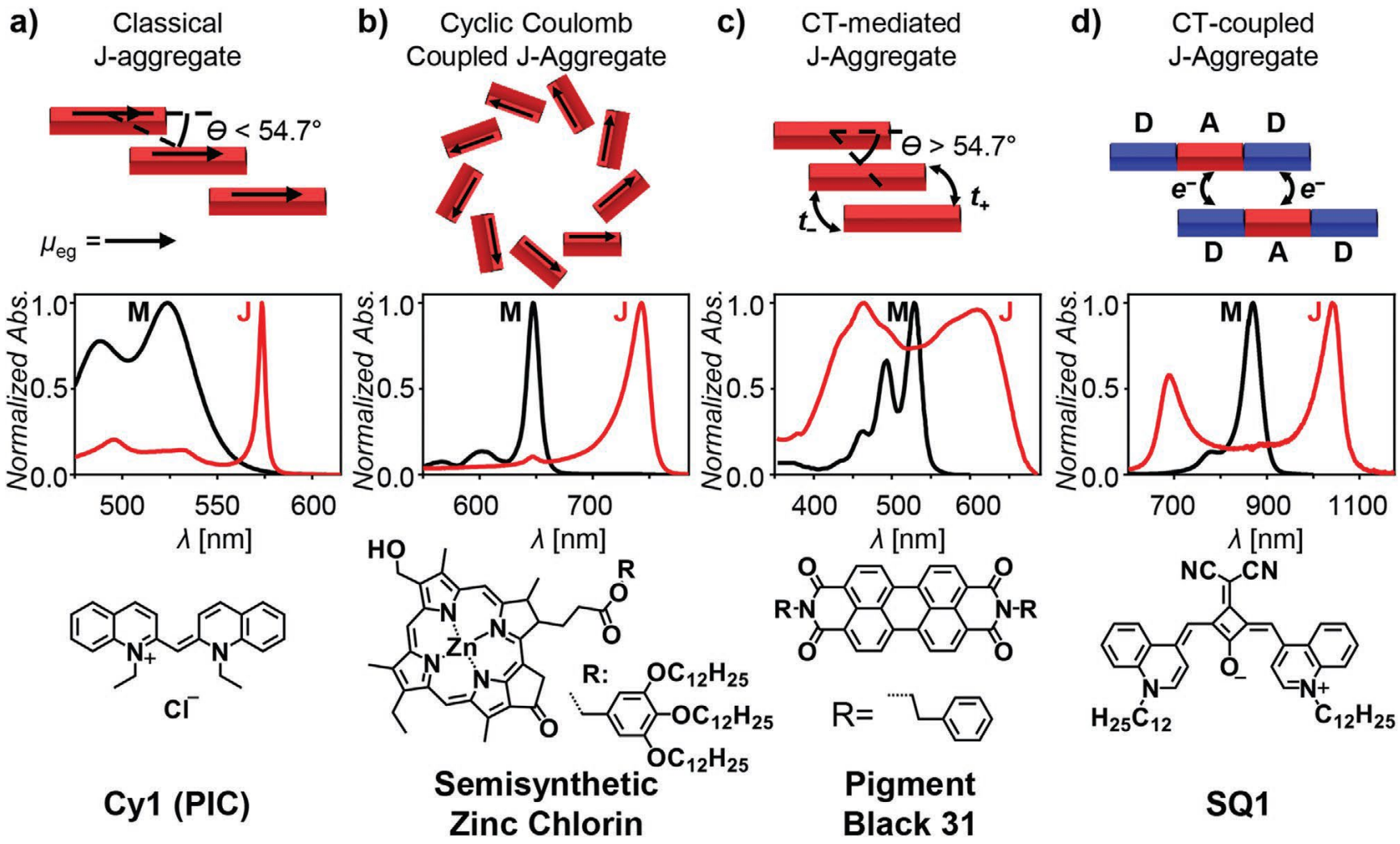

J. H. Kim, Adv. Mater. **2021**, 2104678

Charge transfer excitons

$$E_{CT} = E_{D+A-} + \lambda_{D+A-}$$

$$E_{D+A-} = E_{LUMO,A} - E_{HOMO,D}$$

λ_{D+A-} is the reorganisation energy

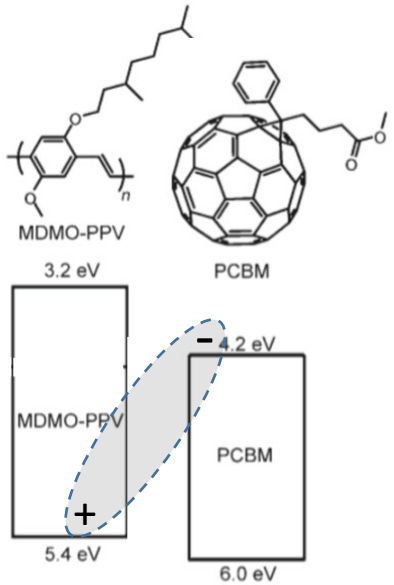

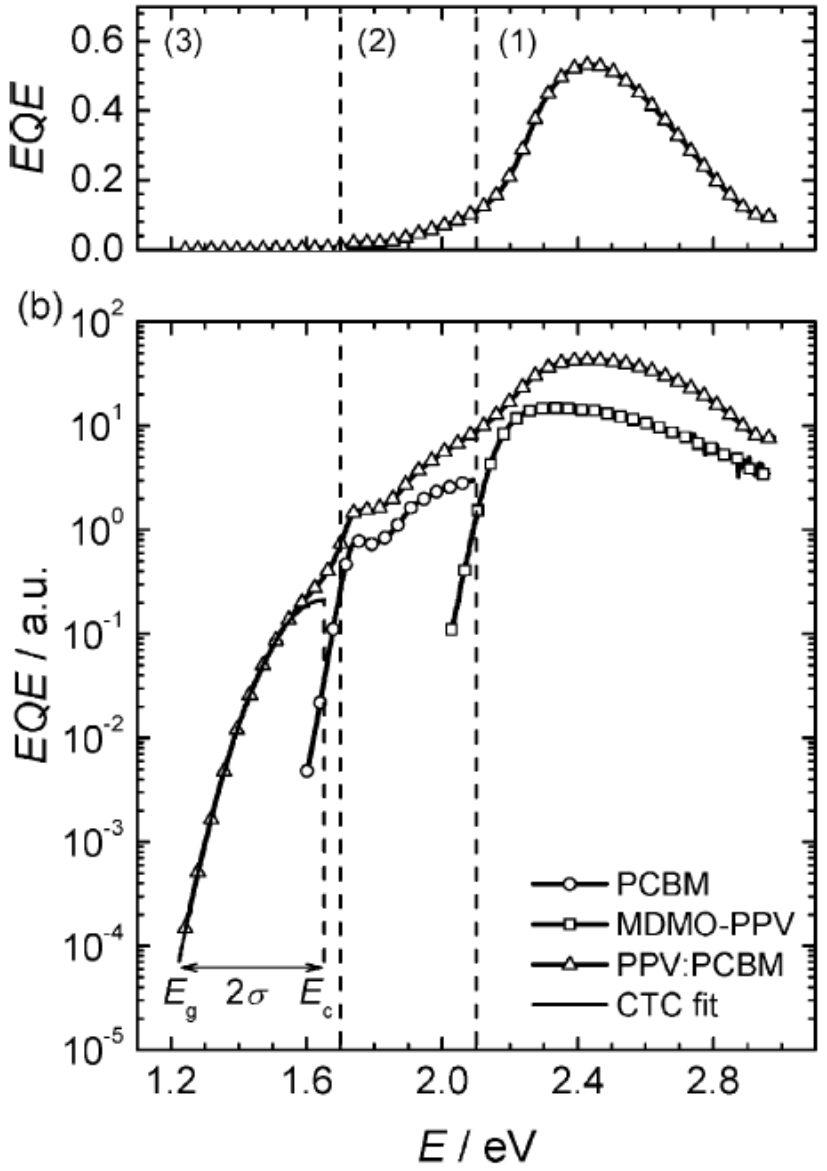

Adv. Funct. Mater. 2008,18, 2064–2070

Diffusion of excitons

Within its lifetime t, the exciton is able to move in a homogeneous material in a random walk fashion. The microscopic driving force for diffusion is nonradiative energy transfer, which can be either Förster transfer (singlet excitons) or Dexter transfer (singlet and triplet excitons). The mean separation between the starting point and the end point is

$$L_D = \sqrt{ZD\tau}$$

where Z is 2,4 or 6 for 1D, 2D and 3D systems, respectively. The diffusion constant D in one dimension is defined by $J_D = -D\,\partial n/\partial x$ and n is the exciton density. The unit of D therefore is cm^2/s.

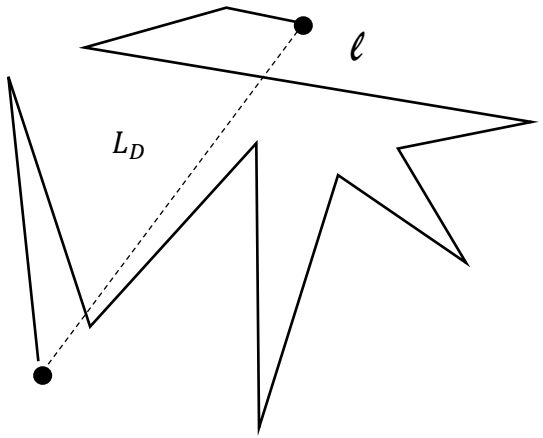

For a normal diffusion process, the exciton density varies according to:

$$\frac{\partial n}{\partial t} = D\Delta n - \frac{n}{\tau}$$ where τ is the lifetime of the exciton.

Here we examine the diffusion process induced by Förster energy transfer

$$k_F(d) = \frac{1}{\tau_{hop}} = \frac{1}{\tau_{fluo}}\left(\frac{R_0}{d}\right)^6$$

where $1/\tau_{hop}$ is the hopping frequency of the exciton between the chromophores, τ_0 is the intrinsic exciton lifetime that is not limited by any quenching processes and d is the distance between the chromophores, R_0 is the Förster radius, as given before in the lecture:

$$r_0^6 = \frac{0.529\kappa^2\phi_{PL}}{n^4 N_A}\int F(\bar{\nu})\varepsilon(\bar{\nu})\frac{d\bar{\nu}}{\bar{\nu}^4} \qquad \kappa = cos\theta_{12} - 3cos\theta_1 cos\theta_2$$

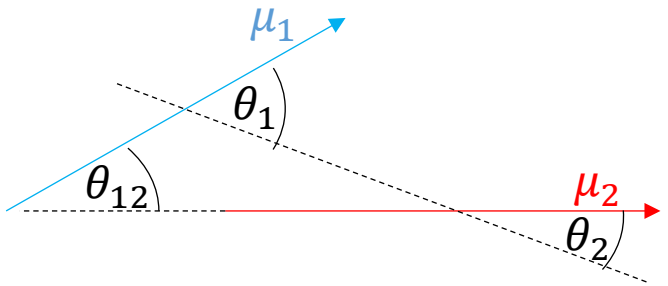

The angles can be inferred from the figure on the left for in-plane transition dipole moments, $0 \leq \kappa^2 \leq 4$. The Förster energy transfer rate becomes zero, when the two transition dipole moments μ_1 and μ_2 are perpendicular to one another. For randomly oriented dipoles $\kappa^2 = 2/3$.

The exciton diffusion coefficient *D* can be estimated using the Smoluchowski–Einstein theory of random walks:

$$D = \frac{d^2}{6\tau_{hop}} = A\frac{1}{\tau_{fluo}}\left(\frac{R_0^6}{6d^4}\right)$$

A is a coefficient taking account of the different length distributions d. Using the FRET expression for R_0 , the diffusion length can now be expressed as:

$$L_D = \sqrt{\tau_{exc} D} = \frac{1}{d^2\sqrt{6}}\sqrt{\frac{A\cdot 0.529\kappa^2}{n^4 N_A}\frac{\phi_{PL}}{\tau_{fluo}}\int F(\bar{\nu})\varepsilon(\bar{\nu})\frac{d\bar{\nu}}{\bar{\nu}^4}}$$

Diffusion length in amorphous materials

In an isotropic material with small intermolecular distances and a strong oscillator strength, the diffusion length for singlet excitons can be as high 100 nm (this limit was calculated for tetracene single crystals). However, in reality, there is energetic disorder and there is first a so-called downhill diffusion, meaning that states with lower energy are populated and diffusion proceeds via thermally activated hopping:

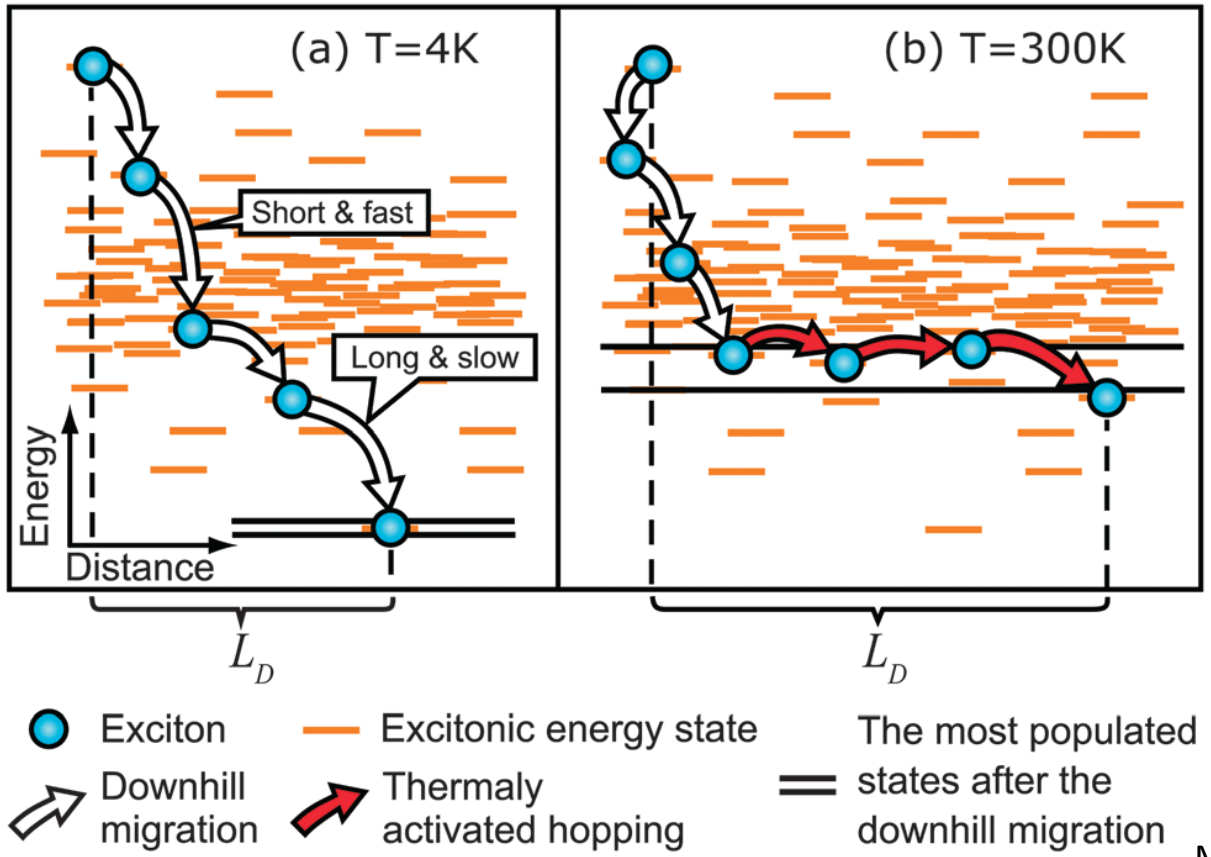

M. Anni, M. E. Caruso, S. Lattante and R. Cingolani, J. Chem. Phys., 2006, 124, 134707

Singlet exciton diffusion length in typical amorphous and polycrystalline materials

Table 3 Measured values of singlet exciton diffusion length and diffusion coefficient (❖ polycrystalline, O amorphous, α thermally annealed, → temperature dependence measured)

Material[a]	1D L_D (nm)	D ($cm^2\ s^{-1}$)	Method	Comment	Ref.
$(C_{12}OCH_2)_8PcH_2$	10–20		PL quenching	O	262
1-NPSQ	2.9		Spectrally resolved PL quenching	O	189
4P-NPD	4		LED remote sensing	O	222
6T	60		PL quenching in bi-layers	❖→	186
Alq3	3–25	$(3–2000) \times 10^{-6}$	Exciton–exciton annihilation; PL quenching; photocurrent	O→	110, 170, 176, 181, 263 and 264
ASSQ	11		Spectrally resolved PL quenching	O	189
BEH-PPV	6.5	2×10^{-3}	PL quenching in bi-layers	O	171
BP	15		Photocurrent	❖	218
C–PCPDTBT	6		PL quenching in blends	O	190
C_{60}	5–40		Photocurrent, microwave conductivity	O	55, 210 and 215
$C_6PT_1C_6$-DPP	12.9	9.4×10^{-4}	Various techniques	❖	121
C_6PT_2-DPP	2–5	$(0.3–1.1) \times 10^{-4}$	PL quenching in blends	Oα	234
$C_6PT_2C_6$-DPP	9.2	3.9×10^{-4}	Various techniques	O	121
CoPc	1.4		Photocurrent	O	63
CPB	16.8		PL quenching in bi-layers		114
CuPB	2		Photocurrent	❖	218
CuPc	5–15, and 68		Photocurrent	❖	55, 63, 219, 265 and 177
Dendrimers	8–17	$(1.8–4.3) \times 10^{-3}$	PL quenching in bi-layers	O	183
DIP	16–100	5×10^{-3}	PL quenching in bi-layers, photocurrent	❖O→	114, 223 and 233
DPASQ	10.7		Spectrally resolved PL quenching	O	189
DTS$(FBTTh_2)_2$ aka T1	3–7	$(3–5) \times 10^{-4}$	PL quenching in blends	Oα→	65 and 195
$EHPT_2C_6$-DPP	7.4	4×10^{-4}	Various techniques	O	121
$F_{12}TBT$	11		PL quenching in bi-layers	O	182
F8BT	8–12	5.3×10^{-4}	PL quenching in blends, and bi-layers	O	182 and 195

Energy Environ. Sci., 2015, 8, 1867--1888

Triplet exciton diffusion length in typical amorphous and polycrystalline materials

Table 4 Measured parameters of triplet exciton diffusion. (□ single crystal, ❖ polycrystalline, ○ amorphous, → temperature dependence measured)

Material[a]	1D L_D (nm)	D ($cm^2\ s^{-1}$)	Method	Comment	Ref.
$(C_{12}OCH_8)_8PcZn$	23	9×10^{-8}	Annihilation	❖	208
$(C_{18}OCH_2)PcH_2$	64	1.6×10^{-5}	Annihilation	❖	207
1,4-Dibromonaphtalane	8400	3.5×10^{-4}	annihilation, delayed PL	□	272
4P-NPD	11–54		Remote sensing in LED configuration	○	53 and 238
Alq3	14–140	$(0.8–7.2) \times 10^{-7}$	Remote sensing in LED configuration, annihilation, delayed PL	○	44,140,273
Anthracene	610 and 7000–20000	$(0.5–2) \times 10^{-4}$	Annihilation, delayed PL, direct imaging	□ →	67, 246, 248 and 274–277
C_{60}	28–35		Photocurrent, PL quenching	○	200 and 217
CBP	8.3–300	$(1.4–770) \times 10^{-8}$	Remote sensing in LED configuration, PL quenching, photocurrent	○	143, 239, 244, 278 and 279
F8-F6	50	7.9×10^{-6}	Annihilation	○	259
F8-PDA	41	4.7×10^{-6}	Annihilation	○	259
$Ir(ppy)_3$-cored dendrimers	2–10	$(8–400) \times 10^{-9}$	Annihilation	○	243
mCP	16		Remote sensing in LED configuration	○	237
Naphthalene	35000	3.3×10^{-5}	Annihilation, delayed PL	□	272
NPD	6–87		Photocurrent, remote sensing in tri-layers.	○	240 and 258
P(CM-Ru_x)	36	$(1–200) \times 10^{-7}$	PL quenching in bi-layers	○	247
PCBM	21	4.2×10^{-6}	PL quenching in blends	○	200
PdTPPC	30	8×10^{-7}	Microwave conductivity	○	242
Pentacene	40–800	$(1–4) \times 10^{-3}$	Annihilation, transient absorption, PL quenching, photocurrent	□❖	6, 9, 14 and 280
PF		3×10^{-4}	Transient absorption	○	260
$Ph_{95}BTD_5$	22	4.7×10^{-6}	PL quenching in blends	○	200
PhLPPP	1700–3900	$(0.5–14) \times 10^{-6}$	Transient absorption, annihilation, phosphorescence	○→	101 and 245
Pt acetylide oligomers		1.8×10^{-4}	Transient absorption	○	281
PtOEP	13–30		Quenching in bi-layers and blends	○	114, 200 and 254
Pyrene	1200	1.3×10^{-4}	Annihilation, delayed PL	□	282
Rubrene	1000–4000		Photocurrent, direct imaging	□	5 and 187
Stilbene	11000	9×10^{-5}	Annihilation, delayed PL	□	272
Super Yellow PPV	10		Quenching in bi-layers	○	241
Tetracene	100–400	$(0.1–1.6) \times 10^{-4}$	Photocurrent, annihilation, delayed PL	□	151, 255, 256 and 283

Exciton transport in molecular aggregates

PIC J-aggregate (Jelly, Scheibe, 1936)

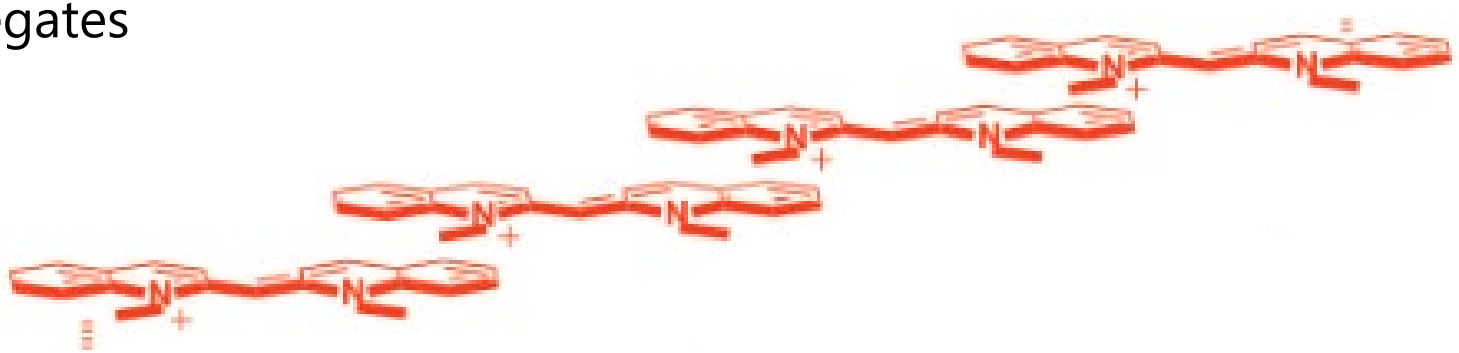

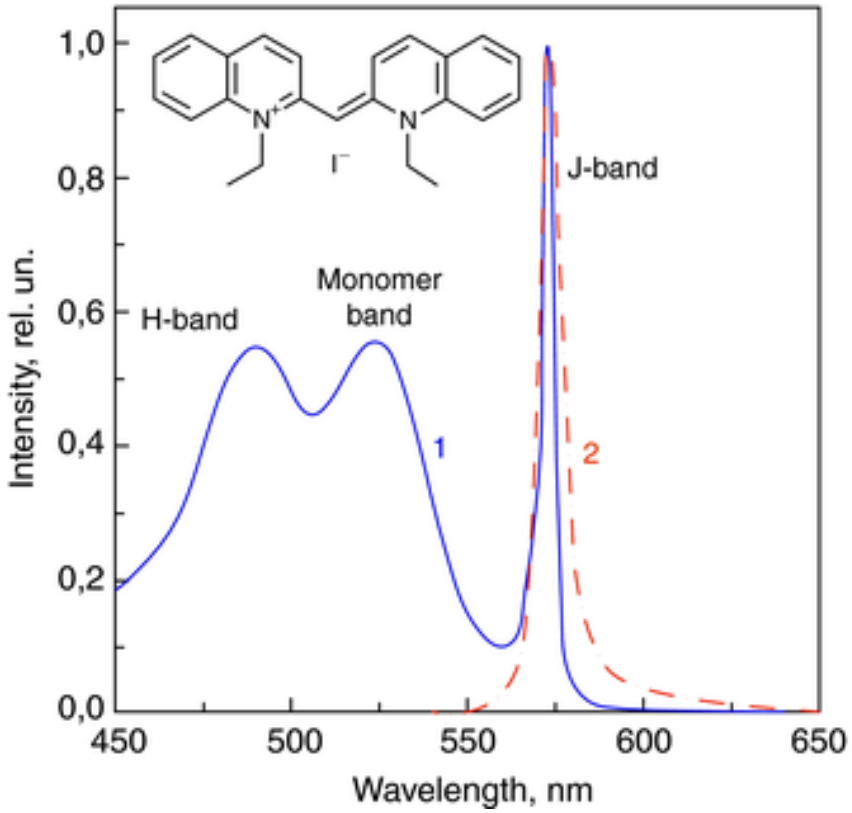

J. AM. CHEM. SOC. 2008, 130, 17114–17119

Exciton coherence length

$$N_{\mathrm{del}}^{W} = \sqrt{\frac{3\pi^2|J|}{W}} - 1, \qquad W = \frac{3\pi^2|J|}{(N_{\mathrm{del}}+1)^2}.$$

N_{del}^{W} is the number molecules across which the exciton is delocalized
J is the exciton coupling energy
W is the bandwidth at half maximum (HWHM)

Journal of Luminescence 87}89 (2000) 66}70

$$\frac{I_{0-0}}{I_{0-1}} = \frac{N_{coh}}{S}$$

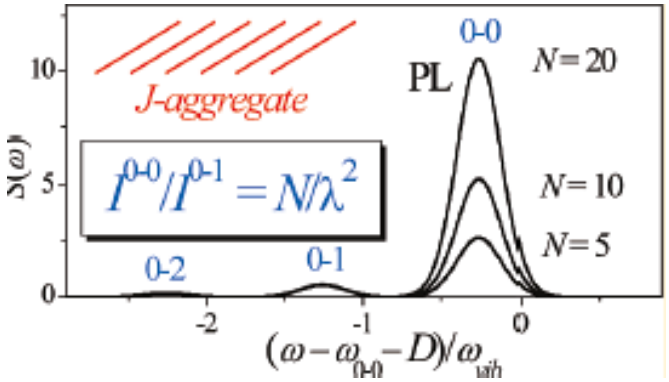

N_{coh} is the coherence length in terms of number of molecules
S is the Huang-Rhys parameter

F. Spano et al., J. Phys. Chem. B 2011, 115, 5133–5143

$$N_{\mathrm{del}} = \frac{3(\Delta\nu_{\mathrm{FWHM}}^{\mathrm{mon}})^2}{2(\Delta\nu_{\mathrm{FWHM}}^{\mathrm{J}})^2} - 1$$

N_{del} is the coherence length in terms of number of molecules
Δ_{FWHM}^{J} is the bandwidth of the J-aggregate
Δ_{FWHM}^{mon} is the bandwidth of the monomer

N_{del} is about 10 molecules.

J. Phys. Chem. C, Vol. 113, No. 29, 2009

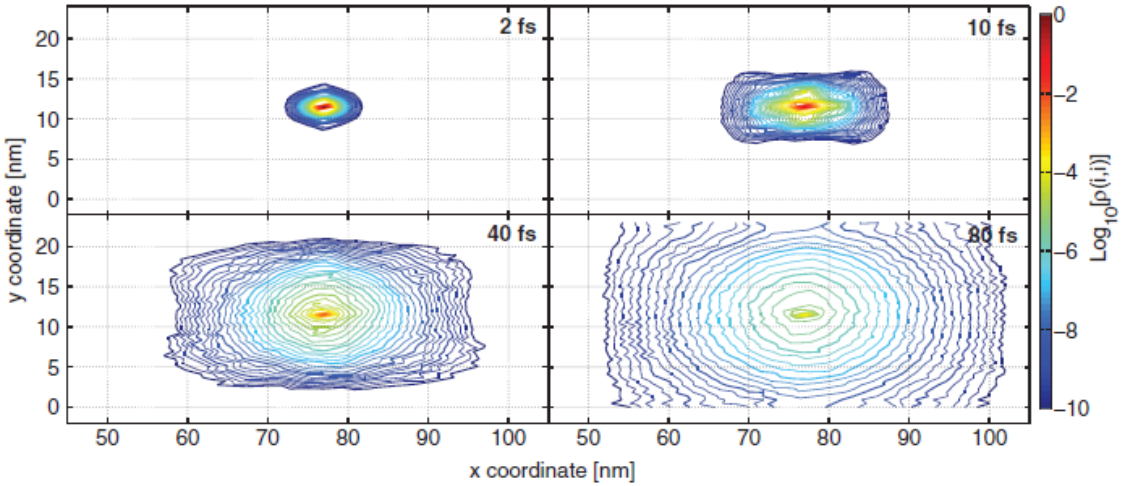

Monte Carlo study of coherence dynamics as a function of static and dynamic disorder.

S. Valleau et al., J. Chem. Phys. 137, 034109 (2012)

Exciton-exciton anihilation to measure exciton diffusion lengths

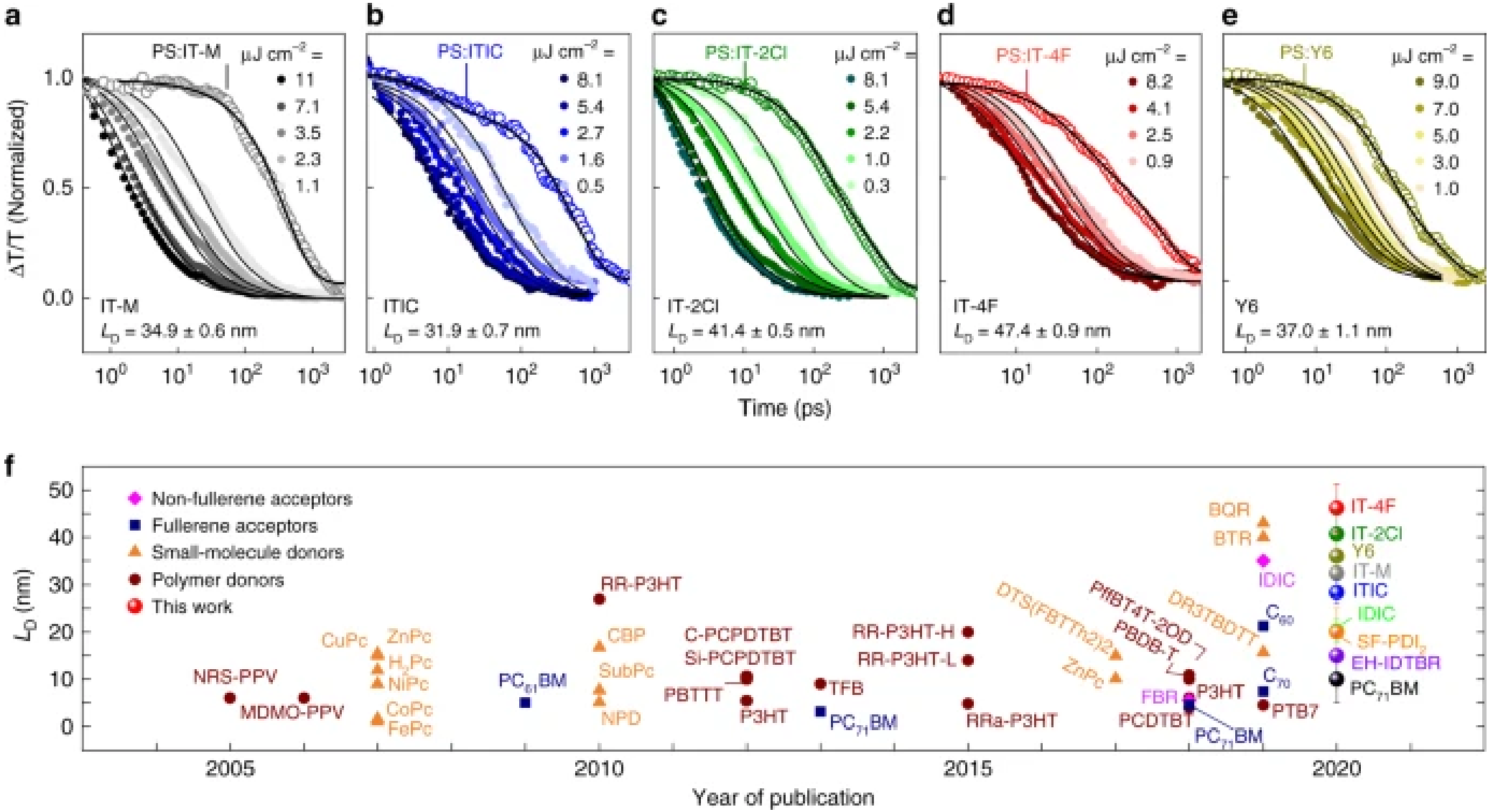

NATURE COMMUNICATIONS | (2020) 11:5220

The analysis involves a fitting to the rate equation:

$$\frac{dn(t)}{dt} = kn(t) - \frac{1}{2}\alpha n(t)^2$$ with solution:

$$n(t) = \frac{n(0)e^{-kt}}{1 + \frac{\alpha}{2\kappa}n(0)[1 - e^{-kt}]}$$

$k = 1/\tau$ is the fluorescence rate, τ is the lifetime
α is the bimolecular exciton annihilation rate in units of $cm^3 s^{-1}$.

The diffusion constant is obtained from :

$$D = \frac{\alpha}{8\pi R}$$

R is the annihilation radius and is usually taken as 1nm.
The diffusion length is then obtained from :

$$L_D = \sqrt{D\tau}$$

An additional estimation of the diffusion constant in one-dimensional aggregates uses the Fermi golden rule:

$$k_{ET} = \frac{1}{2\hbar}|V|^2 J(\varepsilon) = \frac{1}{\hbar^2 c}|V|^2 J(\bar{\nu})$$

V is the exciton coupling energy.
$J(\bar{\nu})$ is the normalized spectral overlap integral between the absorption and emission spectrum.

From the random walk hopping model in 1 dimension we have:

$$D = k_{ET}\frac{a^2}{2} = \frac{a^2}{2}\frac{1}{\hbar^2 c}|V|^2 J(\bar{\nu})$$

a is the interstice hopping distance (distance between molecules in the aggregate)

J. Phys. Chem. A 2011, 115, 648–654

Triplet-Triplet fusion

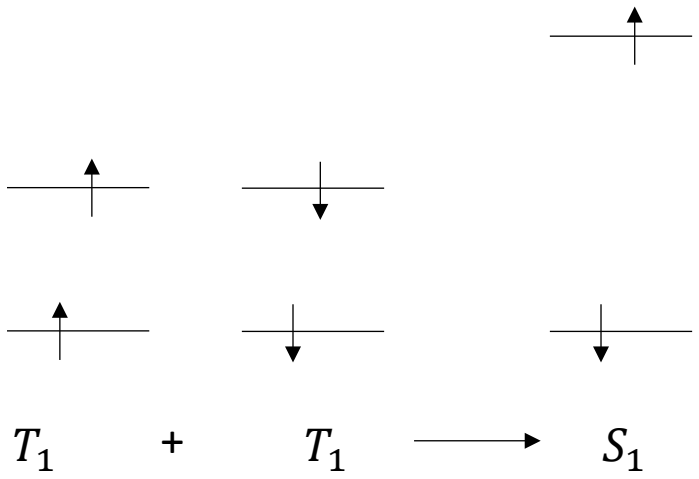

- The fusion process is only allowed for the $^1(TT)$ complex , but may proceed via intermediate $^3(TT)$ and $^5(TT)$ states.
- The energy of two triplet excitons lies slightly above the singlet exciton energy: $2E(T_1) \approx E(S_1)$
- Long triplet lifetimes lead to higher fusion efficiency
- Most efficient materials are tetracene based
- This process may be exploited in OLEDs and OPV

Triplet-triplet fusion can be used for light upconversion. In the work below, a triplet sensitizer was used to transfer triplet states to tetracene, where the fusion occurs.

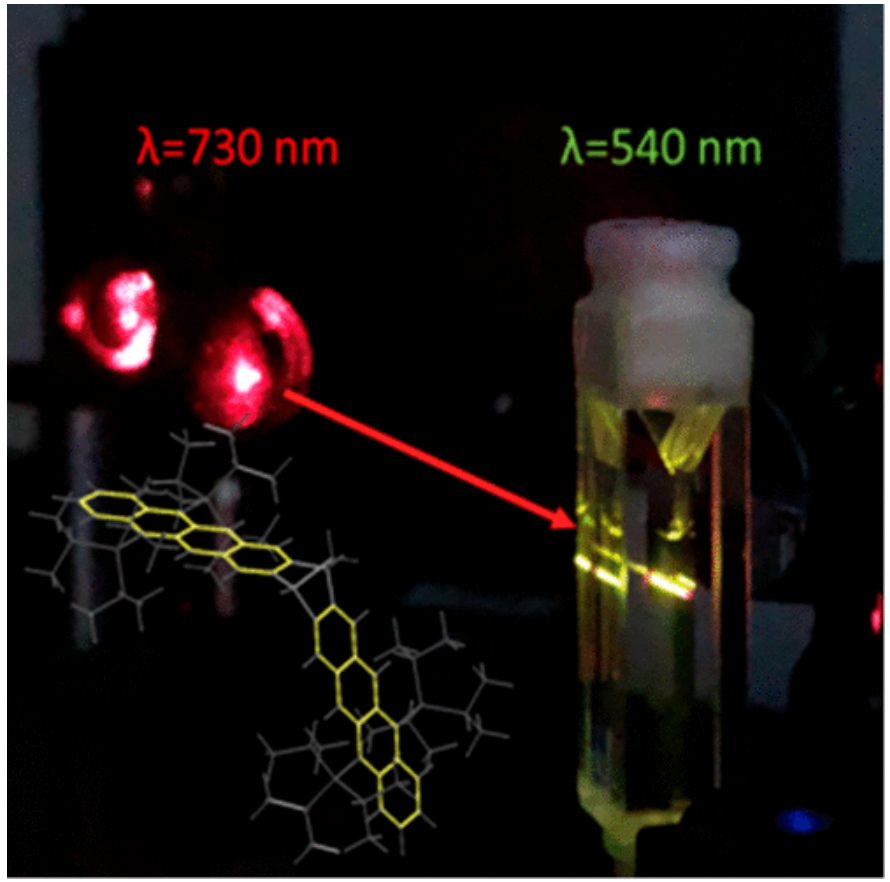

J. Phys. Chem. Lett. 2019, 10, 7463−7469

Singlet fission

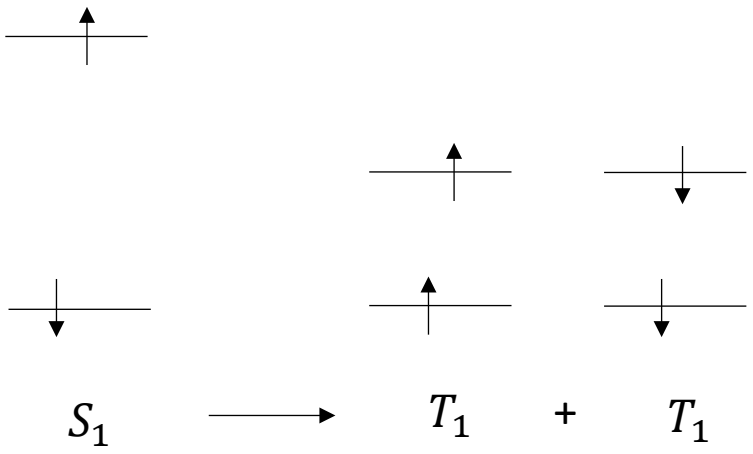

- The fission process is only allowed to form via the $^1(TT)$ complex, which then needs to dissociate in free triplet states
- The limiting processes are triplet fusion and TT annihilation
- Enhancement of free triplet formation can occur through a spatially separated extended ^{1}(T…T) state intermediate (see structure to the right)
- The energy of two triplet excitons lies slightly below the singlet exciton energy: $2E(T_1) \leq E(S_1)$
- This effect may be exploited in solar cells with a maximum power conversion efficiency of 45% as compared to 33% for the Shockley Queisser limit for single junction cells.

J. Phys. Chem. Lett. 2019, 10, 7463−7469

A molecular oligomer design enhances the separation of triplet states from each other. A free triplet generation of 124% could be achieved for tetramers.

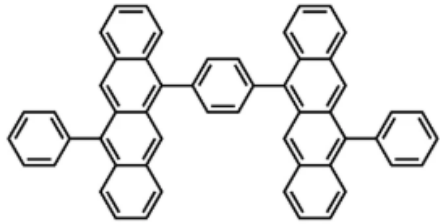
Dimer

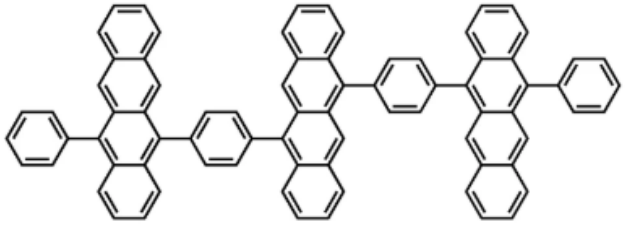
Trimer

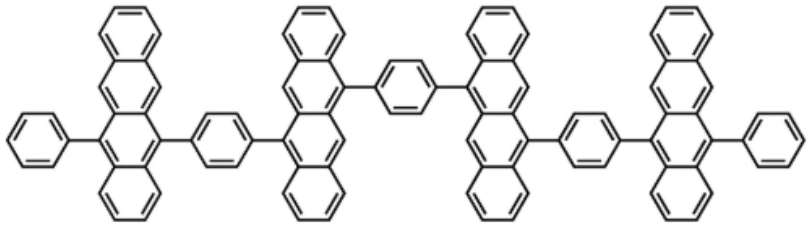

Nature Chemistry | VOL 13 | June 2021 | 559–567